ACTA TECNOLOGÍA

electronic journal
ISSN 2453-675X
Volume 6
Issue 3
2020

International Scientific Journal about Technologies

CONTENTS
(SEPTEMBER 2020)

Acta Tecnología - International Scientific Journal about Technologies
Volume: 6 2020 Issue: 3 Pages: 59-67 ISSN 2453-675X

doi:10.22306/atec.v6i3.78 *Received: 26 Apr. 2020; Revised: 11 June 2020; Accepted: 19 Sep. 2020*

OPTIMIZATION AND MATERIAL CHARACTERIZATION OF GROUNDNUT SHELL AND RICE HUSK FOR PRODUCTION OF PARTICLEBOARD

Olawale Olamide
Chemical Engineering Department, Landmark University, Km 4 Ipetu, Omu-Aran Road,
PMB 1001, Ipetu Road, Omu-Aran, Kwara State, Nigeria,
olawale.olamide@lmu.edu.ng (corresponding author)
Akinyemi Banjo
Agriculture and Biosystems Engineering, Landmark University, Km 4 Ipetu, Omu-Aran Road,
PMB 1001, Ipetu Road, Omu-Aran, Kwara State, Nigeria, akinyemi.banjo@lmu.edu.ng
Attabo Favourite Omojo
Chemical Engineering Department, Landmark University, Km 4 Ipetu, Omu-Aran Road,
PMB 1001, Ipetu Road, Omu-Aran, Kwara State, Nigeria, attabo.favouriteomojo@lmu.edu.ng

Keywords: particle board, urea formaldehyde, groundnut shell, rice husk, optimization
Abstract: The aim of this work is to the produce particle board (PB) from groundnut shell and rice husk using optimization approach. This research is tailored towards the quest for economical and eco-friendly materials by converting a waste into wealth. Box Behnken Design was used to optimize the effect of three variables: Groundnut husk (0-100g); Rice husk (0-100g) and resin (1.5-2.5g) respectively. The optimal process levels predicted by the software for the PB were validated. The PB produced was analysed using Scanning Electron Microscope. The best levels from the interactions of the variables were: groundnut husk:50g; rice husk:100g and resin:3.50 with MOR of 3.50 N/mm^2 and MOE of 932.4 N/mm^2 while the predicted optimal levels of 65.99g; 86.34g and 1.69 was validated .The result of the Validation gave MOR of 3.49 N/mm^2 and MOE of 932.10 N/mm^2 . It can be concluded that particle board produced at the optimized conditions satisfied the American National Standard ANSI/A208.1-999 specification for general purpose particle boards.

1 Introduction

The demand for wood in the forest industry has escalated, but the production of industrial wood from the natural forest continues to deteriorate, and increasing concerns for waste minimization have however led to account of the use of agricultural waste in the manufacturing of some construction products. Due to the increase in wood consumption, the reserves of indigenous species of plants have been declining, resulting in a quest for fresh lignocellulose products that can fulfil the requirement effectively. Any lignocellulose material can be used as a raw material for the manufacture of particleboards. Besides wood, agricultural residues such as: cereal straw, sugar cane bagasse, cornstalks and corn cobs, cotton stalks, rice husks, sunflower stalks and hulls among others can be used [1]. A particle board is an engineering wood product produced under pressure using wood chips, sawmill shavings or even sawdust (fibreboard products) with an adhesive binder [2]. However, in developing nations such as Nigeria, the panel / board sector has witnessed constant development in past few years and has recently estimated demand for wood and wood produced panels / boards to be 4.704 and 0.688 million m^3 respectively. This has put a lot of pressure on forest assets leading to deforestation and its associated negative environmental effects as well as higher timber prices [3]. It was reported that the worldwide demand of particleboard panels was 56.2 Mm^3 in 1998 as reported by Food and Agricultural Organization (FAO)of the nation's [4]. The demand for particleboards in the sectors of housing construction and furniture manufacturing has continued to increase [5-6]. Particleboard is a composite panel product made up of wood particles such as sawdust, wood chips, sawmill shavings or other agricultural waste related to synthetic resin or other suitable additive under heat and pressure [7]. It is widely used as flooring material, wall bracing, ceiling boarding, furnishings, partitioning, cladding and so on. Composite materials are manufactured by mixing two or more materials to enhance the original's characteristics. There is a chance that two or more lignocellulose materials would be coupled for more valuable products without affecting the particle board's properties. In latest years, the manufacturing of composite materials from agricultural wastes as an alternative particleboard to timber-based products has become a major study area [8]. Several of these lignocellulose components have been used to effectively create inorganic-bonded boards, particle boards and fibre boards to some extent.

The composite material's particles are held together by synthetic resins and other additives may be added to enhance the properties of the final composite material. Several resin kinds are widely used with the cheapest and easiest to use being urea formaldehyde and phenol formaldehyde resin [9]. One of the major causes of environmental pollution is the rapid depletion as a raw material of forest resources. To reduce forest consumption, it is vital to explore alternative sources of raw materials. It is therefore crucial to explore the suitability for panel (wood) manufacturing of agricultural residues. The use of agricultural waste as a particulate board is eco-friendlier and can aid to promote the concept of waste to prosperity in the construction sector. This will also help to protect the environment and promote environmentally friendly techniques [10]. As sources of environmentally friendly, non-toxic and cheap particle boards, agricultural waste residues have continued to gain attention. Several research reports of the use of agricultural residues for particleboard development exist, such include [11] who explored the manufacturing of coffee husk and hull fibre particle boards using portion-produced thermosetting resins. However, [12] evaluated the impact of adhesive type and loading on the quality of the produced particle board. They reported that the finest particleboard was generated at a load of 6% using urea formaldehyde. Furthermore [13] studied the characteristics of wheat straw and its particleboard manufacturing potential while [8] examined the factors affecting the manufacturing of maize cobs particle boards.

Limited studies however exist on the use of multiple agricultural residues as constituent material in production of composite particleboards. Some of the studies that considered optimization approach for mechanical features of particle boards using Response Surface Methodology are [14-15] considering board density, resin loading and agro-residue quantity as variables. The outcome obtained showed that the mechanical features (MOE and MOR) were affected by the volume of resin and agro-residue used but did have any significant effect on the MOE and MOR of the boards produced. In the same vein, [16] studied the impact of process parameters on the tensile characteristics of groundnut shell-vinyl ester composites using experiment design analysis. Three process parameters were considered namely: particle size, filler processing, and alkaline particle therapy. Tensile characteristics were predicted using surface response methodology and the findings showed that the tensile strength and tensile modulus increase with increase in filler loading up to 50-wt% and beyond 5% NaOH treatment of particles. To the best of the authors' knowledge, limited studies have attempted to optimize the characteristics of the particleboard produced from these agrarian residues. While studies on the mechanical conduct of agricultural waste based particleboards have been recorded in the literature, restricted research has been reported on the impact of control variables such as the amount of agro-residue composite and urea formaldehyde resin on the mechanical properties of the particle boards. Hence, this research investigated the use of groundnut shell and rice husk as a composite for the production of particle board using optimization approach.

2 Materials and Methods

2.1 Materials

The materials used for this research were groundnut shell (GS) and Rice Husk (RH) which were collected from Landmark University commercial farm and lastly the binder (Urea Formaldehyde Resin) was also sourced locally.

2.2 Experimental Design

The experimental settings were designed using Response Surface Methodology (RSM). It was conducted using Box-Behnken design in the software Design Expert (6.0.8). This was used to determine the effect of the interactions of the three variables, which are: GS, RH and resin loading on the mechanical properties of the particle boards produced. The range and levels of the independent variables are as shown in Table 1. The matrix for the three variables were varied at 3 levels (-1, 0 and +1) as shown in Table 2.

Table 1 Coded and actual levels of the factors for three factor Box-Behnken design for particle board production

Independent Variables	Independent Variables			
	Symbols	-1	0	+1
Independent Variables	X_1	0	50	100
Independent Variables	X_2	0	50	100
Independent Variables	X_3	1.5	2.0	2.5

Table 2 Design Matrix for the Production of Particle Board from Groundnut Shell and Rice Husk

	Coded variables				Groundnut husk	Rice husk	Resin
					Actual Variables		
Std	Run	X_1	X_2	X_3	X_1	X_2	X_3
16	1	1	-1	0	100	0	2.0
7	2	0	1	-1	50	100	1.5
9	3	0	0	0	50	50	2.0
12	4	0	1	1	50	100	2.5
4	5	0	-1	-1	50	0	1.5
11	6	1	0	1	100	50	2.5
8	7	-1	0	-1	0	50	1.5
14	8	-1	0	1	0	50	2.5
5	9	-1	-1	0	0	0	2.0
17	10	1	0	1	100	50	1.5
10	11	0	0	0	50	50	2.0
1	12	0	0	0	50	50	2.0
15	13	0	-1	1	50	0	2.5
13	14	0	0	0	50	50	2.0
6	15	1	1	0	100	100	2.0
3	16	-1	1	0	0	100	2.0
2	17	0	0	0	50	50	2.0

The Box-Behnken design has been established to be suitable for the quadratic response surfaces and this design generated a second-degree polynomial model [16].

As shown as:

$$Y_i = b_0 + \sum b_i X_j + \sum b_{ij} X_i X_j + \sum b_{ii} X_i^2 + e_i \text{ .... (1)}$$

Where Y_i is the dependent variable or predicted response, X_i and X_j are the independent variables, b_0 is the offset term, b_i and b_{ij} are the single and interaction effect coefficients and e_i is the error term.

The Design Expert software was used for regression and graphical analysis of the experimental data. The optimum values of the variables tested were obtained by numerical optimization based on the criterion of desirability [17]. The responses analysed were MOE and MOR respectively. Design matrix for the production of PB from GS and RH is shown in Table 2.

2.3 Production of Particle Boards

The groundnut shell was washed to remove debris and other foreign materials present in it. It was further air dried at 23 °C for 2 days after washing to reduce moisture content and further milled for size reduction. The GS and RH were sieved and separated into two different sizes (0.85 mm and 1.7 mm) using standard sieve sizes. Required composition and weight as determined by the experimental design was measured and poured into a mixing bowl. Based on the optimization protocol, the needed resin dosage was added and the mix was manually mixed homogenously for about 3 minutes until the required uniformity was attained.

Thereafter, the mixture was transferred to 80 x 120 x 300 mm wooden mould with the interior covered with polyethene material. Standard tamping rod was used to compact the PB before the cover was placed and put under a cold press at 3.8 MPa for 24 hours and later hot pressed for 6 hours. The particle board produced after moulding is as shown in Plate 1. Samples of 10 x 60 x 150 mm needed for physical and mechanical tests were cut from the PB and 3 replications were performed for proper analysis.

2.4 Mechanical Test

Modulus of Elasticity (MOE) and Modulus of Rupture (MOR) were conducted in accordance with [18-19] for Testing Materials methods for evaluating properties of wood base fibre and particle panel material using Universal Testing Machine. Both properties were calculated from the following equations:

$$MOR = \frac{3PL}{2bh^2} \text{ ....(1)}$$

$$MOE = \frac{PL^3}{4bh^3Y} \text{ ....(2)}$$

where: P = maximum load or maximum force, L = span, b = width, h = thickness and Y = deflection.

2.5 Characterization of Particle Board and thermal conductivity

The scanning electron microscope (SEM) was used to observe the morphology of the particle board. SEM was used to examine the microstructural morphology occurring at the surface of the boards and chemical composition of the boards following wetting and drying. Furthermore**,** Electron Dispersive Spectroscopy (EDS) was used to determine the elemental composition of the particle board produced. A Hot Disk Thermal Constants Analyzer, which uses the transient plane source method, was employed to measure the thermal conductivity of the various samples. All tests were conducted under ambient environmental conditions (20–22 °C).

3 Results and Discussion

Box-Behnken design for Response (MOR and MOE) is as shown in Table 3.

Table 3 Box-Behnken design for Response (MOR and MOE) production of particle boards

Run	Coded Factors			Actual Values			MOR(N/mm^2) Response		MOE(N/mm^2) Response	
	X_1	X_2	X_3	X_1	X_2	X_3	Actual	Predicted	Actual	Predicted
1	1	-1	0	100	0	2.0	2.28	2.25	576.5	599.0
2	0	1	-1	50	100	1.5	3.50	3.69	932.4	946.0
3	0	0	0	50	50	2.0	2.45	3.19	732.4	822.3
4	0	1	1	50	100	2.5	2.14	2.10	360.8	429.5
5	0	-1	-1	50	0	1.5	0.43	0.47	492.5	423.8
6	1	0	1	100	50	2.5	1.74	1.96	680.2	671.3
7	-1	0	-1	0	50	1.5	2.99	2.77	764.7	773.6
8	-1	0	1	0	50	2.5	2.36	2.38	678.0	631.8
9	-1	-1	0	0	0	2.0	2.13	2.31	494.2	554.0
10	1	0	-1	100	50	1.5	3.38	3.86	760.1	806.3
11	0	0	0	50	50	2.0	3.38	3.19	845.0	822.3
12	0	0	0	50	50	2.0	3.38	3.19	844.3	822.3
13	0	-1	1	50	0	2.5	0.47	0.27	677.1	663.5
14	0	0	0	50	50	2.0	3.38	3.19	845.0	822.3
15	1	1	0	100	100	2.0	5.10	4.92	794.0	734.2
16	-1	1	0	0	100	2.0	4.66	4.69	729.6	707.1
17	0	0	0	50	50	2.0	3.38	3.19	845.0	822.3

The equations (3) and (4) were obtained from the response via the regression analysis in terms of coded terms. The response generated in terms of coded and predicted values for both MOR and MOE is as shown below:

$$MOR = 3.01 + 0.50X_1 + 1.01X_2 + 1.85X_3 + 0.036X_1X_2 - 0.18X_1X_3 - 0.24X_2X_3 + 0.33X_1^2 - 0.16X_2^2 - 1.24X_3^2 \ldots\ldots\ldots\ldots \quad (3)$$

$$MOE = 891.5 - 3.93X_1 + 123.29X_2 + 9.06X_3 - 2.19X_1X_2 + 1.19X_1X_3 - 132.33X_2X_3 - 16.84X_1^2 - 68.31X_2^2 - 67.23X_3^2 \ldots\ldots\ldots\ldots \quad (4)$$

Table 4 showed the ANOVA for MOR while Table 5 showed ANOVA for MOE respectively. Furthermore, Table 4 and 5; revealed that the models for MOR and MOE were statistically significant with p values of 0.0004 and 0.0057 respectively as shown in Tables (4) and (5). However, the models showed that the terms: representing the amount of GS and RH and the resin loading were significant showing that all variables influenced the MOR and MOE of the boards produced.

Table 4 ANOVA results for model representing MOR

Sources	Sum of squares	DF	Mean Squares	F value	P value
Model	23.65	9	2.63	19.67	0.0004
X_1	1.07	1	1.07	8.00	0.0255
X_2	4.31	1	4.31	32.26	0.0008
X_3	3.07	1	3.07	22.98	0.0020
X_1X_2	0.021	1	0.021	0.16	0.7034
X_1X_3	0.26	1	0.26	1.91	0.2096
X_2X_3	0.49	1	0.49	3.67	0.0970
X_{12}	1.86	1	1.86	13.96	0.0073
X_{22}	0.42	1	0.42	3.17	0.1184
X_{32}	6.50	1	6.50	48.61	0.0002
Residual	0.94	7	0.13		
Lack of Fit	0.24	3	0.081	0.47	0.7200
Pure Error	0.69	4	0.17		
Cor Total	24.59	16			

Table 5 ANOVA results for model representing MOE

Sources	*Sum of Squares*	*DF*	*Mean Square*	*F Value*	*P value*
Model	3.397	9	37745.94	8.13	0.0057
X_1	65.38	1	65.38	0.014	0.9089
X_2	64224.00	1	64224.00	13.83	0.0075
X_3	73.29	1	73.29	0.016	0.9036
X_1X_2	80.10	1	80.10	0.017	0.8992
X1X3	11.56	1	11.56	2.189	0.9616
X_2X_3	1.43	1	1.430	30.77	0.0009
X_{12}	4970.26	1	4970.26	1.07	0.3354
X_{22}	81829.27	1	81829.27	17.62	0.0041
X_{32}	19032.46	1	19032.46	4.10	0.0826
Residual	32517.55	7	4645.36		
Lack of Fit	22405.68	3	7468.56	2.95	0.1613
Pure Error	10111.87	4	2527.97		
Cor Total	3.72	16			

F Value of 19.67 for MOR and 8.13 for MOE showed that models generated were significant. Statistical information for ANOVA showed that the models describing MOR and MOE has high coefficient of determination (R^2) as shown in Table 6. This showed that the models were able to adequately represent the relationship between the chosen factors (amount of GS, amount of RH and resin loading) and the responses (MOR AND MOE). R^2 values of 0.96 and 0.91 means that the models were able to explain 96% and 91% of the variability observed in the values of MOR and MOE respectively. The values obtained showed a high reliability as recommended by Montgomery [17]. The adequate precision for both models indicated that the models can be used to navigate design space [20].

Table 6 Statistical information for ANOVA

Parameter	**MOR value**	**MOE value**
R-Squared	0.96	0.91
Mean	2.77	708.93
Standard Deviation	0.37	68.16
C.V %	13.18	9.61
Adeq. Precision	16.57	9.99

3.1 Results of 3D Surface Plots

Figure 1 showed the effect of resin loading and the amount of groundnut shell on the MOR of the particle boards. The trend observed showed that MOR increased with increase in the amount of the resin and the amount of groundnut shell simultaneously.

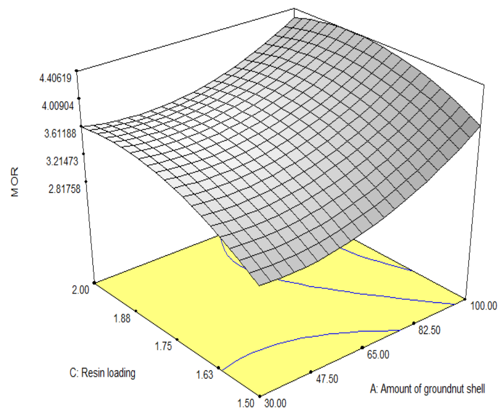

Figure 1 Effect of amount of Rice husk and amount of groundnut shell on MOR

This showed that there was appropriate adhesion between the amounts of groundnut shell. Previous reports have shown that to produce particle boards with high MOR, more of the resin has to be used. According to report by [21]; the mechanical and physical properties of particle boards could be enhanced by increasing the amount of resin used. The resin loading has been reported to determine the amount of voids present in the boards produced [8]. However, when low amounts of resin are used, the resin is mixed up with the agro residue particles leaving some voids present. However, when the resin loading is increased, some of it is mixed up with the agro residue particles to form the finish while the remainder fills up the voids that would otherwise be present in the finished product. Intermediate amounts of both groundnut shell and rice husk was needed to produce particle boards with high MOR values meaning that more resin could be used to produce the boards therefore resulting in the improvement of the mechanical properties. The effect of resin loading and amount of rice husk on the MOR is shown in Figure 2. Furthermore, Figure 3 showed that high MOE values were obtained when low levels of rice husk were used. The resin loading did not significantly influence the MOR of the boards.

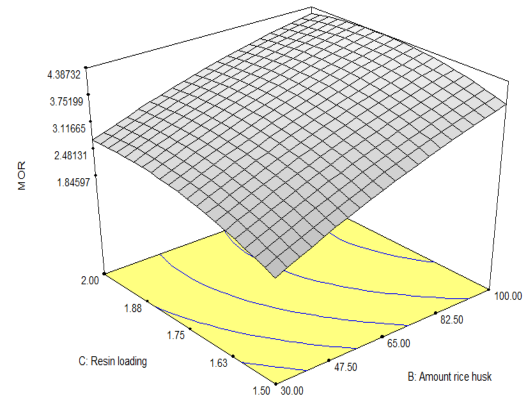

Figure 2 Effect of resin loading and amount of groundnut shell on MOR

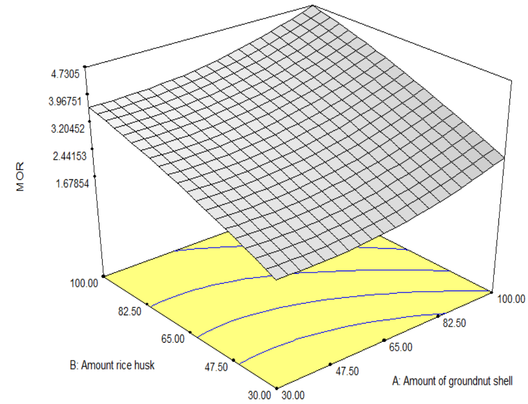

Figure 3 Effect of resin loading and amount of rice husk on MOR

The MOE of the boards was observed to increase with increase in the amount of rice husk as shown in Figure 4. The MOE of the boards was observed to increase with increase in resin loading as shown in Figure 5. Good bond quality resulting from adequate contact between the resin and the agro residue particles has been cited as a reason for high MOE values ([8]. This is because high resin loadings increase the bond contact between the particles which in turn results in improved surface contact [22]. Since MOR and MOE are both mechanical properties, the trend observed for both would be expected to be similar. Both measures of mechanical strength of particle boards have been reported to be influenced by particle geometry and amount of resin. The requirement for agro residue-based particle boards is high MOR and MOE. Figures 5 and Figure 6 showed that high MOE values were obtained when low levels of agro residue were used. Since a fixed ratio of agro residue to resin was utilized in producing the boards, a low level of agro residue translates to a high loading of resin. Therefore, reducing the amount of agro residue means increasing the amount of resin used which consequently increases the MOE of the boards. [23] reported that the increase in content of resin viscosity helps in enhancing the bonding strength.

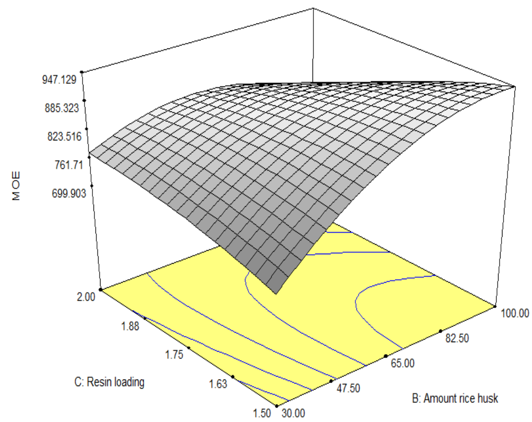

Figure 4 Effect of amount of rice husk and amount of groundnut shell on MOE

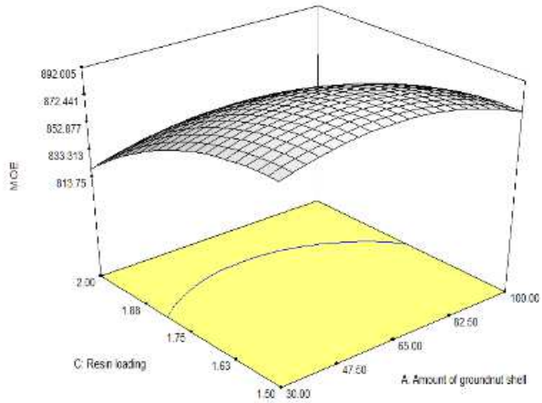

Figure 5 Effect of resin loading and amount of groundnut shell on MOE

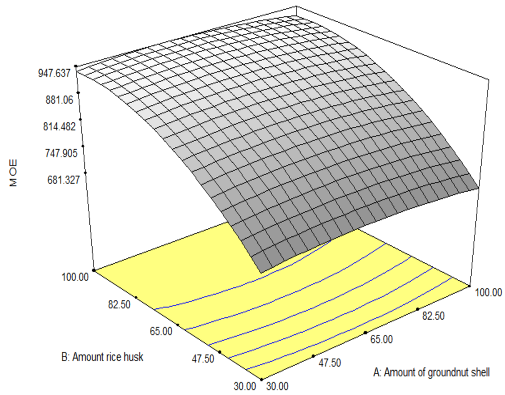

Figure 6 Effect of resin loading and amount of rice husk on MOE

3.2 *Validation of Optimal Predicted Levels*

The optimal variables predicted by the software which was validated as given in Table 7. The result showed that the maximum MOR and MOE values of 3.50 N/mm^2 and

932.40N/mm^2 respectively obtained were close to the predicted values of 3.49 N/mm^2 and 932.10 N/mm^2 respectively which confirmed result by [22]; of 0.50 to 1.40 N/mm^2 for binder-less particleboard made from oil palm trunk. The excellent correlation between the predicted and measured values of these experiments shows the validity of the statistical model. Good correlation between experimental and the predicted results confirmed adequacy of the model predicted.

Table 7 Optimal variables validated

S/N	Amount of groundnut shell	Amount of rice husk	Resin loading	MOR	MOE	Desirability
1	65.99	86.34	1.69	3.49	932.10	1.000

3.3 *Scanning Electron Microscopy (SEM) and EDS Analysis*

The particle board from both the best process level and validated were subjected to SEM and the results observed showed that the surface of the boards showed fibrous network structures which were covered and bonded by the resin. The boards with the higher resin loading had lower voids because the resin is cured more effectively in the void spaces in Figure 7. The lower density board in Figure 8 has higher voids and spaces which results in high moisture absorptivity. The density of the board is found to increase with increasing resin loading.

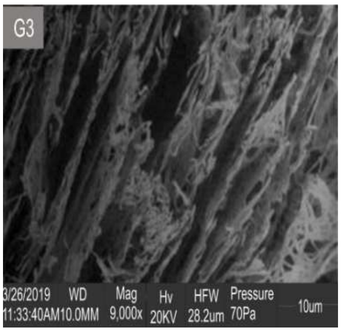

Figure 7 Particleboard from best process level

The Energy Dispersive X-ray Spectroscopy (EDS) was carried out to study the percentage of elements. The variation of percentage of elements suggests inhomogeneity in molecular composition such as organic or inorganic composition. The table below (Table 8) shows the variations of the percentage of elements.

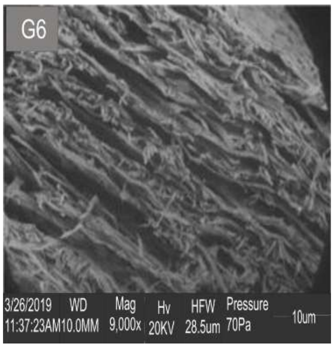

Figure 8 Validated particleboard

Table 8 Energy Dispersive X-ray Spectroscopy results

Samples	C	0	K	Si	Ca	Mg	Na	Al
G3	3.20	51.30	8.51	34.65	1.23	3.50		0.10
G6		52.39	3.02	24.04	8.92	1.02	8.60	1.45

3.4 *Thermal Properties Analysis*

The result of the thermal conductivity is as shown in Table 9. The heat flow transfers through solid substance and void, while the thermal conductivity of air within the voids is much lower than that of solid substance, therefor a lower thermal conductivity of the whole material. Thus, the lower density boards conduct less heat than the higher density boards. From Table 9, the higher the density of the board, the higher the thermal conductivity of the boards but due to a close difference between their densities, the values of the thermal conductivity were slightly different. Furthermore, densities of 367, 375 kg/m^3, then the values of the thermal conductivity are 0.172, 0.178 W/mK respectively.

Table 9 Thermal Conductivity results

Parameter	Thermal Conductivity (W/mK)
G3(Particleboard from best process level)	0.172
G6 (Validated)	0.178

4 Conclusion

Design of experiment for response surface methodology has been demonstrated to be useful in optimizing the board production process. Mechanical properties of the boards such as MOR and MOE were influenced by the amount of agro residue and resin used.

Quadratic statistical models developed to represent MOR and MOE showed a good fit with the experimental data with R^2 values of 0.96 and 0.91 respectively. The predicted optimum conditions of; 65.99 g of groundnut shell, 86.34 g of rice husk and 1.69 g of resin loading was validated to give a MOR and MOE of 3.50 N/mm^2 and 932.40 N/mm^2. The particle board produced at the optimized conditions satisfied the American National Standard ANSI/A208.1-1999 specification for general purpose particle boards. This study showed that particle boards were produced from groundnut shell and rice husk using urea formaldehyde as binder. It can be concluded that optimizing the agricultural waste products and the resin was successful for the production of particle boards.

References

[1] FIORELLI, J, SARTORI, D.L., CRAVO, J.C.M., SAVASTANO, H. jr., ROSSIGNOLO, J.A., NASCIMENTO, M.F.: Sugarcane bagasse and Castor oil polyurethane adhesive-based particulate composite, *Materials Research*, Vol. 16, No. 2, pp. 439-446, 2013. doi:10.1590/S1516-14392013005000004

[2] ROWELL, R.M.: *Handbook of Wood Chemistry and Wood Composites*, CRC press, 2012.

[3] SOTANNDE, O.A., OLUWADARE, A.O., OGEDOH, O., ADEOGUN, P.F.: Evaluation of cement-bonded particle board produced from Afzelia africana wood residues, *Journal of Engineering Science and Technology,* Vol. 7, No. 6, pp. 732-743, 2012.

[4] YOUNGQUIST, J.A., HAMILTON, T.E.: *A look at the world's timber resources and processing facilities*, In: Proceedings of the XXI IUFRO World Congress 2000, Sub-plenary sessions, vol. 1, Kuala Lumpur, Malaysia: pp. 183-190, 2000.

[5] SELLERS, T.: Growing markets for engineered products spurs research, *Wood Technology*, Vol. 127, No. 3, pp. 40-43, 2000.

[6] AHMED, E., DAS, A.K., HANNAN, M.O., SHAMS, M.I.: Particleboard from coir pith, Bangladesh Journal of Scientific and Industrial Research, Vol. 51, No. 3, pp. 239-245, 2016.

[7] OBAM, S.O.: Properties of saw-dust, paper and starch composite ceiling board, *American Journal of Scientific and Industrial Research*, Vol. 3, No. 5, pp. 300-304, 2012.

[8] SEKALUVU, L., TUMUTEGYEREIZE, P., KIGGUNDU, N.: Investigation of factors affecting the production and properties of maize cob-particleboards, *Waste and Biomass Valorization*, Vol. 5, No. 1, pp. 27-32, 2014.

[9] AKINDAPO, J.O., BINNI, A.U., SANUSI, O.M.: Development of Roofing Sheet Materials using Groundnut Shell Particles and Epoxy Resin as Composite Material, *American Journal of Engineering Research,* Vol. 4, No. 6, pp. 165-173, 2015.

[10] BEKTAS, I., GULER, C., KALAYCIOĞLU, H., MENGELOGLU, F., NACAR, M.: The manufacture of particleboards using sunflower stalks (Helianthus annuus l.) and poplar wood (Populus alba L.), *Journal of Composite Materials,* Vol. 39, No. 5, pp. 467-473, 2005.

[11] BEKALO, S.A., REINHARDT, H.W.: Fibers of coffee husk and hulls for the production of particleboard, *Materials and Structures,* Vol. 43, pp. 1049-1060, 2010.

[12] MENDES, R.F., MENDES, L.M., JÚNIOR, J.B.G., SANTOS, R.C.D., BUFALINO, L.: The adhesive effect on the properties of particleboards made from sugar cane bagasse generated in the distiller, *Revista de Ciências Agrárias*, Vol. 32, No. 2, pp. 209-218, 2009.

[13] BOQUILLON, N., ELBEZ, G., SCHONFIELD, U.: Properties of wheat straw particleboards bonded with different types of resin, *Journal of Wood Science,* Vol. 50, pp. 230-235, 2004.

[14] AMENAGHAWON, N.A., OSAYUKI-AGUEBOR, W., OKIEIMEN, C.O.: Production of particle boards from corn cobs and cassava stalks: Optimization of mechanical properties using response surface methodology, *Journal of Materials and Environmental Science*, Vol. 7, No. 4, pp. 1236-1244, 2016.

[15] AMENAGHAWON, N.A., OGBEIDE, S.E., OKIEIMEN, C.O.: Application of Statistical Experimental Design for the Optimization of Dilute Sulphuric Acid Hydrolysis of Cassava Bagasse, *Acta Polytechnica Hungarica*, Vol. 11, No. 9, pp. 239-250, 2015.

[16] RAJU, G.U., KUMARAPPA, S., GAITONDE, V.N.: Study on effect of process parameters on tensile properties of groundnut shell-Vinyl ester composite: Analysis using Design of Experiment, *International Journal of Materials Science and Engineering*, Vol. 3, No. 3, pp. 193-207, 2015.

[17] MONTGOMERY, D.C.: *Design and Analysis of Experiments*, 6 ed., New York: John Wiley & Sons, Inc, 2005.

[18] ASTM D 1037-06a (American Society for Testing Materials), Standard test methods for evaluating properties of wood-based fiber and particle panel materials static tests of timbers, D 1037- 93, ASTM, Philadelphia, PA, 1999.

[19] ANSI A208.1, Particleboard. American National Standard, National Particleboard Association, 2009.

[20] CAO, G., REN, N., WANG, A., LEE, D.J., GUO, W., LIU, B., FENG, Y., ZHAO, Q.: Acid hydrolysis of corn stover for biohydrogen production using Thermoanaerobacterium thermosaccharolyticum W16, *International Journal of Hydrogen Energy,* Vol. 34, No. 17, pp. 7182-7188, 2009.

[21] MURAKAMI, K., UEDA, M., MATSUDA, H., ZHANG, M., KAWASAKI, T., KAWAI, S.: Manufacture and properties of three-layered particleboards with oriented face strands of veneers,

I. Effects of face strand/core article ratios, Resin types and resin contents on the board properties, *Japan Wood Research Society,* Vol. 45, No. 5, pp. 395-402, 1999.
[22] BABATUNDE, B., OLUFEMI, D.: Properties of cement-bonded flake boards from Gmelina arborea Leucaena leucocephala, *International Journal of Biological and Chemical Sciences*, Vol. 5, No. 2, pp. 586-594, 2011.
[23] DERKYI, N.S.A, SEKYERE, D., DARKWA, N.A., YARTEY, J.G.: Effect of cassava flour as Urea-formalidehyde Adhensive extender on the bonding strength of plywood, Ghana, *Journal of Forestry*, Vol. 23, pp. 25-34, 2008.

Review process

Single-blind peer review process.

doi:10.22306/atec.v6i3.84 *Received: 01 May 2020; Revised: 14 June 2020; Accepted: 10 Aug. 2020*

DESIGN OF THERMOPLASTIC IMMOBILIZATION FOREARM SPLINTS

Maria Danko
Technical University of Košice, Department of Biomedical Engineering and Measurement, Letna 9, 042 00 Košice, Slovak Republic, EU, maria.danko@tuke.sk
Monika Michalikova
Technical University of Košice, Department of Biomedical Engineering and Measurement, Letna 9, 042 00 Košice, Slovak Republic, EU, monika.michalikova@tuke.sk
Lucia Bednarcikova
Technical University of Košice, Department of Biomedical Engineering and Measurement, Letna 9, 042 00 Košice, Slovak Republic, EU, lucia.bednarcikova@tuke.sk
Marianna Trebunova
Technical University of Košice, Department of Biomedical Engineering and Measurement, Letna 9, 042 00 Košice, Slovak Republic, EU, marianna.trebunova@tuke.sk (corresponding author)
Martina Nalevankova
Technical University of Košice, Department of Biomedical Engineering and Measurement, Letna 9, 042 00 Košice, Slovak Republic, EU, martina.nalevankova@tuke.sk
Radovan Hudak
Technical University of Košice, Department of Biomedical Engineering and Measurement, Letna 9, 042 00 Košice, Slovak Republic, EU, radovan.hudak@tuke.sk

Keywords: thermoplastic, splints, design, forearm, orthoses
Abstract: A retrospective view of orthopaedic devices gives the impression of a missing element. Fully functional custom-made orthoses appear to be prototypes in progress. They lack colour, variety, original motif, uniqueness, additional functionality i.e. design. Nowadays it is possible to choose a colour combination of the whole orthosis and the aim of the submitted study is to find out the interest in incorporating an additional function or original design.

1 Introduction, study background

If we focus on small children, teenagers or adolescents who need to be motivated to wear orthoses, the solution offers custom made design [1,2]. Little girls would welcome iridescent orthoses with glittering sequins and a large unicorn, the "boys" would not disdain the comic motif of their sci-fi action hero, which would also attract the looking of people around [3,4]. From a practical point of view, especially with long-term wear during the day [5], a splint with an USB key, a smart watch or a small transcript text field on the forearm would be helpful.

In order to create a statistical survey of the present study, the area of investigation is focus on the specific type of forearm brace that is one of most often orthopaedic aid used after trauma, surgeries, illnesses etc [5]. Therefore, this article is focused on a custom-made thermoplastic immobilization splint for the dorsal side of the hand, which is applied to about 75% of the forearm and 50% of the hand causes. This fixation positioning device prevents wrist flexion and is made of a low-temperature thermoplastic, that can be arbitrarily shaped, modelled and applied to any part of the body after heating [5-7]. So, this is a fast and net production with minimal patient discomfort with the benefits of being lightweight and well ventilated [5,8,9]. It allows easy deployment and composition, e.g. personal hygiene [10]. Indications for prescription are mostly injuries and hand surgery. It is prescribed when the joints are dislocated, sprain and stretched ligaments. According to the ŠÚKL Code, it is classified like a therapeutic instrument that is prescribed or dispensed according to the patient's health condition, otherwise once a year or compensatory paid by the health insurance company once a year. Individually made passive brace of the hand is fully paid by the health insurance company. If the client does not have health insurance or a doctor's prescription, as it also has a prescription restriction (OPR, ORT, CHI, TRA, RHB), it can be made for a direct payment, depending on the price list of a particular orthopaedic manufactory. Most also offer special and extra adjustments for an additional fee [11-14].

2 Methods

The aim of the presented study is to evaluate the merits of incorporating a functional or original element on a thermoplastic splint of forearm. At the Department of Biomedical Engineering and Measurement it was made several designs with some improvements that were tested by general population of physiologically and mentally healthy people, that were divided into four categories according to ontogenetic development [3].

Acta Tecnología - International Scientific Journal about Technologies
Volume: 6 2020 Issue: 3 Pages: 69-72 ISSN 2453-675X

The study sample consists of 60 respondents divided into four age groups [3]:

1. small children and schoolchildren aged 3-12 years, 9 respondents, nurseries and pupils
2. adolescents aged 13-20 years, 32 respondents, pupils and students
3. adults aged 21-64, 17 respondents, doctoral students and teachers
4. seniors aged 65 and over, 2 respondents, pensioners

The survey is based on a questionnaire and was focused on a purely lay, theoretical assessment of the added value of individual handmade original pieces. None of the respondents surveyed has experience with the long-term use of an immobilization thermoplastic splint. Therefore, for the purpose of this study and better imagination the splint would be for a non-dominant limb and the period of use of the fixation brace for 16 hours per day for 6 months [5]. The most important question was if the design and the additional functions of the orthosis are important to respondents. They were able to choose from following design and it was allowed to point more than one option.

2.1 Variants of design for thermoplastic splints from the questionnaire

A) Hand painted splints

The design of the brace is truly custom made, with the only limitations being the artist's fantasy and creative abilities. Pictures of splints from our department with own motives e.g. street art for “little” superheroes, car track, design inspired by Japanese geisha or for girl with ladybugs and many more (Figure 1).

Figure 1 Hand painted splints

B) Choose from samples of colour and pattern

There is also a wide range of colours, patterns and finishes available on the manufacturer's websites (Figure 2).

Figure 2 Samples of colour and pattern

C) Splint „Whiteboard surface with white board pen“

The surface of the splints is especially adapted for repeated writing and erasing with the added marker pen (Figure 3).

Figure 3 Splint „Whiteboard surface with white board pen“

D) Brace with alarm, GPS or with smart watch

The device can make an alarming sound or send a mobile phone signal to an ICE person or measure vital signs or for sport training and other (Figure 4).

Figure 4 Brace with alarm

E) Brace "pills always with you"

Splints with practical box for storing valuable treasures for children but also adults e.g. to pills, flash cards and so on (Figure 5).

Figure 5 Brace "pills always with you"

Acta Tecnología - International Scientific Journal about Technologies
Volume: 6 2020 Issue: 3 Pages: 69-72 ISSN 2453-675X

F) Thermoplastic splint with built-in USB key (Figure 6)

Excellent aid not only for pupils and students.

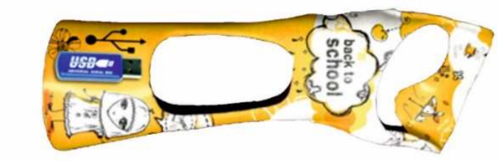

Figure 6 Thermoplastic splint with built-in USB key

G) Standard forearm immobilization splint without custom design (Figure 7)

Figure 7 Standard forearm immobilization splint

3 Evaluation of statistical survey

Respondents were asking about their age and then were categorized accordingly this [5]. They have written all of their experience with orthopaedic devices (to any part of the body) in terms of evaluating their application for a 24 hour mode of action and commenting to the total period of orthotics brace using for months [4]. None of the survey participants had experience with thermoplastic forearm splint at the time of filling in the form.

Each additional element on the brace was evaluated in the questionnaire separately. There were interesting views on the essence of design and interest in associated value depending on the respondent's age. Quantitative representation of design in each category is given by numerical value and evaluation by percentage.

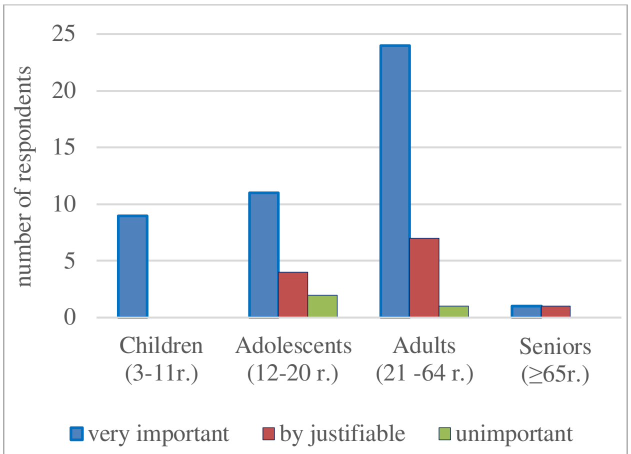

Figure 8 Opinion on the design depending on the age of the respondents

Based on our study sample, design is important, as up to 95% of them responded (see Figure 1), and its need grows exponentially depending on the long-time of use of the orthopaedic device. Because most of the respondents started to think more about the design, when taking into account the temporal aspect of using the orthosis [13,14]. Of course, children definitely want to a colour thermoplastic splint, as up to 100% of them show the necessity of this (see Figure 8) and preferably with their own motif, with magic white board surface, smart watch or USB key (see Figure 9).

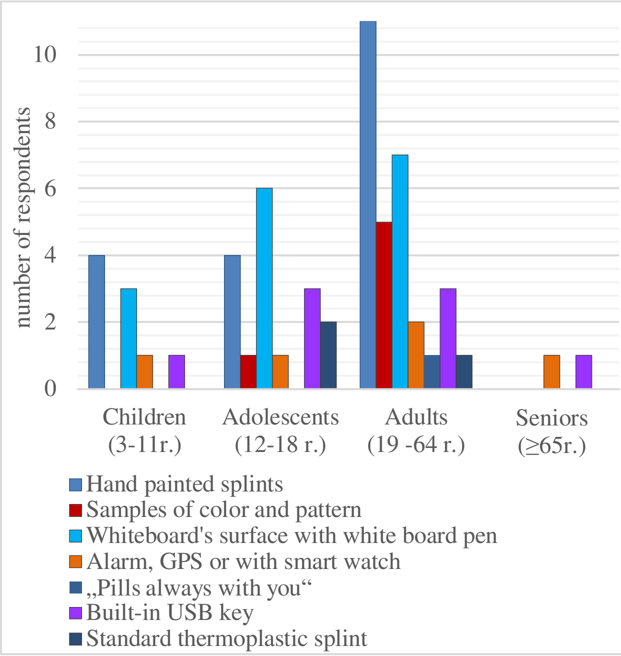

Figure 9 Evaluation of variants of design of thermoplastic splint from the questionnaire

Adolescents would appreciate a splint with a surface of marker board and white board pen (35.3% of them). 23.5% of them would like an original hand painted design or having an USB key always at hand (17.6% of them). Two of the interviewed teenagers and one adult would not be interested in any improvements, they are also not interested in to choose from the sampler of colour or pattern. Up to 40.6% of adults would prefer to self-realize by choosing an original painting or improving the brace for a fashion accessory. Also, up to 21.8% of them would appreciate the surface of whiteboard with white board pen. Seniors would be interested in an orthosis with an alarm or a built-in USB key.

4 Conclusions

The present study examines the merits of design implementation according to the ontogenetic categorization of respondents, using the method of qualitative evaluation based on the subjective opinion of the individual. According to the concept of the survey, the upward trend of a hand-made original with incorporated functional accessories can be clearly stated. The question of comfort was answered by 68% of respondents that they would not mind any restrictions on use resulting from the design in terms of increased caution e.g. sequins, buttons, USB key, button, watch or attached pen etc. Overall, 55% of surveyed the adolescents and adults would not hesitate to pay extra for a possible custom-made redesign. Based on the data obtained from the survey participants, it can be concluded that custom made design has a future and great potential [3-5,13].

Acknowledgement
The work has been supported by research grants KEGA 040TUKE-4/2019, KEGA 041TUKE-4/2019, KEGA 023TUKE-4/2020 and APVV-15-0356.

References

[1] SHAH, P., IFTIKHAR, H., LUXIMON, Y.: *Aesthetic Considerations in the Ortho-Prosthetic Design Process*, Vol 2 No 1 (2019): Conference Proceedings of the Academy for Design Innovation Management: Research Perspectives In the era of Transformations, 2019. doi:10.33114/adim.2019.02.214
[2] FITZPATRICK, A., MOHAMMED, M. I., COLLINS, P., GIBSON, I.: *Design Optimisation of a Thermoplastic Splint*, Solid Freeform Fabrication 2017: Proceedings of the 28th Annual International, Solid Freeform Fabrication Symposium – An Additive Manufacturing Conference, 2017.
[3] NALEVANKOVÁ, M.: *Dizajn ortéz*, Bakalárska práca, Katedra biomedicínskeho inžinierstva a merania (KBIaM), Košice, 2012. (Original in Slovak)
[4] VAZ, F., PRENDEVILLE, S.: *Design as an Agent for Public Policy Innovation*, Conference: Academy for Design Innovation Management 2019 At: London, Conference Paper, 2019.
[5] TAMSIN, M., BACH, Ch.: The Design of Medical Devices, *International Journal of Innovation and Scientific Research*, Vol. 1, No. 2, pp. 127-134, 2014.
[6] JONES, D., WANG, L., GHANBARI, A., VARDAKASTANI, V., KEDGLEY, A.E., GARDINER M.D., VINCENT, T.L., CULMER, P.R., ALAZMANI A.: Design and Evaluation of Magnetic Hall Effect Tactile Sensors for Use in Sensorized Splints, *Sensors*, Vol. 20, No. 4, pp. 1-13, 2020. doi:10.3390/s20041123
[7] YAN, W., DING, M., KONG, B., XI, X., ZHOU, M.: Lightweight Splint Design for Individualized Treatment of Distal Radius Fracture, *Journal of Medical Systems,* Vol. 43, No. 8, pp. 1-10, 2019. doi:10.1007/s10916-019-1404-4
[8] GLUCK, M.J, BECK, C.M, SOCHOL, K.M., LONDON, D.A., HAUSMAN, M.R.: Comparative strength of elbow splint designs: a new splint design as a stronger alternative to posterior splints, *Journal of Shoulder and Elbow Surgery,* Vol. 28, No. 4, pp. 125-130, 2019. doi:10.1016/j.jse.2018.10.015
[9] HWANG, I.S., HUANG C.C., SUL, J.H., HUANG, C.T., WANG, CH., YOUNG, M.S.: The effects of weight load and joint immobilization on reorganization of postural tremor, *Electromyography and Clinical Neurophysiology,* Vol. 46, No. 2, pp. 67-77, 2006.
[10] BARADARAN, A., BARADARAN, A., EBRAHIMZADEH, M.H., KACHOOEI, A.R., RIVLIN, M., BEREDJIKLIAN, P.: Comparison of Custom-made Versus Prefabricated Thumb Splinting for Carpometacarpal Arthrosis: A Systematic Review and Meta-analysis, *The Archives of Bone and Joint Surgery,* Vol. 6, No. 6, pp. 478-485, 2018.
[11] ZENG, T., GAO, D.W., WU, Y.F., CHEN, L., ZHANG, H.T.: Small splint external fixation combined with 3D printing brace for the treatment of Colles fractures, *ZHONGGUO GU SHANG China Journal of Orthopaedics and Traumatology,* Vol. 32, No. 6, pp. 513-518, 2019. doi:10.3969/j.issn.1003-0034.2019.06.006
[12] MEALS, C., CASTRO, N.J., MOSS, D.: Efficient Construction of Volar Wrist Splints: A Biomechanical Study Comparing Splints of Different Material, Thickness, and Design., *Hand (N Y),* Vol. 11, No. 3, pp. 310-313, 2016.
[13] SANDFORD, F., BARLOW, N., LEWIS, J.: A study to examine patient adherence to wearing 24-hour forearm thermoplastic splints after tendon repai rs, *Journal of Hand Therapy,* Vol. 21, No. 1, pp. 44-52, 2008. doi:10.1197/j.jht.2007.07.004
[14] YEO, J.C., LIM, C.T.: Wearable Sensors for Upper Limb Monitoring, *Wearable Technology in Medicine and Health Care,* Vol. 2018, pp. 113-134, 2018. doi:10.1016/B978-0-12-811810-8.00006-3

Review process
Single-blind peer review process.

doi:10.22306/atec.v6i3.85 Received: 01 May 2020; Revised: 14 June 2020; Accepted: 10 Aug. 2020

PROCEDURE FOR THE PRODUCTION OF DYNAMIC PRE-KNEE ORTHOSIS USING THE UNILATERAL SYSTEM

Branko Stefanovic
Technical University of Košice, Department of Biomedical Engineering and Measurement, Letna 9, 042 00 Košice, Slovak Republic, EU, branko.stefanovic@tuke.sk
Monika Michalikova
Technical University of Košice, Department of Biomedical Engineering and Measurement, Letna 9, 042 00 Košice, Slovak Republic, EU, monika.michalikova@tuke.sk
Lucia Bednarcikova
Technical University of Košice, Department of Biomedical Engineering and Measurement, Letna 9, 042 00 Košice, Slovak Republic, EU, lucia.bednarcikova@tuke.sk
Marianna Trebunova
Technical University of Košice, Department of Biomedical Engineering and Measurement, Letna 9, 042 00 Košice, Slovak Republic, EU, marianna.trebunova@tuke.sk (corresponding author)
Jozef Zivcak
Technical University of Košice, Department of Biomedical Engineering and Measurement, Letna 9, 042 00 Košice, Slovak Republic, EU, jozef.zivcak@tuke.sk

Keywords: pre-knee brace, dynamic brace, structural design
Abstract: The article deals with the design of an orthotic solution of dynamic knee orthoses for patients after polio. The aim was to design and create an orthopedic device and describe the technological process of its production. The design, testing and production of the orthosis aim to ensure the physiological position of the foot, to perform plantar and dorsal flexion in the ankle and to verticalize the position of the entire lower limb. These parameters have a considerable impact on maintaining posture, balance, walking stability and locomotion as well as elimination of inappropriate pathological movement habits. The results of orthotherapy show that their use corrects the course of the physiological axis in all planes. The corrected lower limb axis significantly affects the supportive, balance, and allocating ability of individuals.

1 Introduction

At present, the issue of damage to the human musculoskeletal system is increasingly monitored. In terms of the incidence of congenital disorders, an increased number of post-traumatic cases following accidents or injuries, e.g. in traffic accidents, extreme sports, etc., but also in connection with the aging of the population, the demand for orthotic-prosthetic solutions is increasing over time. The phenomenon of aging concerns not only local regions, but also becomes a pan-European and global challenge. Disorders of the musculoskeletal system and deviations from the physiological state thus concern each of us. The impact of lifestyle changes is an integral part of human development and adversely affects the body. It is the changes and diseases of the musculoskeletal system that are closely interconnected with other systems and interact with each other. Orthotics is a narrower specialization of orthopedic prosthetics, which deals with the issue of methods of replacement, or adjustment of lost or weakened functions, prevention and correction of deformities of the musculoskeletal system. The proposal of a particular type of orthosis is processed by an orthopedic technician on the basis of a doctor's recommendation, professional knowledge, skills, and own experience. The final solution is therefore not only dependent on professional competence, but also on a lot of knowledge and examination of professional engineers in the field. This article presents theoretical knowledge of orthotic treatment of knee and ankle disorders by means of dynamic orthoses, as well as practical examples of a particular case - the application of pre-knee dynamic orthosis for a patient after polio.

2 Materials and methods

The article presents two male subjects aged 16 and 18 with dynamic pre-knee braces. Both subjects in childhood have overcome the infectious disease poliomyelitis that attacks the central nervous system (brain and / or spinal cord) [1]. 0.1% of the total number of infections present with permanent paralysis. In these patients, symptoms of post-poliomyelitic syndrome of both lower limbs appear as a result of the disease. Typical images of disability are valgus position of the knees in the frontal plane, hyperextension in the knee joints (Figure 1), dorsal resp. plantar extension of the hinge joints in the sagittal plane [2]. Subjects also exhibit other symptoms such as increased muscle weakness and joint muscle pain, decreased muscle mass (muscular atrophy), increased joint instability / joint deformities and changes in gait patterns, and an increased tendency to fall [3]. All of the above symptoms have a profound effect on the ability to maintain proper posture, balance, gait stability, locomotion as well as the formation of inappropriate pathological movement habits. The present goal is to achieve an improvement in the static attitude and mobility of these subjects by an orthotic solution [4].

Figure 1 Baseline - front side view, subject 1 (left), subject 2 (right)

3 Production of dynamic knee brace

Based on the diagnosis, orthopedic device in the form of dynamic knee orthosis was indicated to both subjects [5]6].

To produce an orthopedic device, it is necessary to measure selected knee length, width and circumferential dimensions by appropriate measuring aids, such as: knee length, knee width, ankle joint width, heel to toe length, forefoot width, foot angle to medial / lateral side, limb circumference - 10 cm above the patella, knee circumference, maximum calf circumference and ankle circumference. If limb discrepancy is present, the limb truncation value should be recorded [7].

After obtaining the necessary dimensional data, the preparation for plastering is started. In this phase of orthopedic device construction, important a line construction points, such as the compromise centre of rotation in the knee joint and the fibula head, are plotted on the limb, which is a load-sensitive location. Other important points are the compromise centre of rotation in the ankle joint, various growths, bone protrusions, painful spots and patella position. On the basis of these substrates a gypsum negative is made by a three-phase procedure (foot negative, knee negative, knee negative) [7].

To keep the load line and the exact location of the orthotic joint, it is advisable to use a plaster stand in which the plaster negative of the lower limb is clamped. The position is corrected on the stand. After all the necessary steps have been taken, the gypsum negates and the gypsum positive (Figure 2) is produced, which must be subsequently treated (correction of casting errors, loadable and non-loadable areas) [7].

Figure 2 Gypsum negative (left) and positives (right) placed in the orthosis stand

3.1 Production of a test orthosis

On the corrected and treated positive, a test orthosis shell (Figure 3) is formed by stretching the high temperature polypropylene thermoplastic heated to 185 ° C with the aid of vacuum suction. For the use of the unilateral lower limb orthosis system, components that are manufactured and classified by patient weight are used. Following are adjustments for the placement of the orthotic joint, shaping the plates, marking the lines of the sleeve edges. The sleeves are removed from the gypsum model and their edges are ground by means of a cylindrical grinder and the surface is smoothed. In the treatment of the longitudinal and angular discrepancies of the limbs, the production of a heel for correction is made by pouring the foil Pedilin, which cures into a solid form. After the foam has hardened, it is ground to the required size, taking into account the axial position of the foot [7].

Figure 3 Test brace assembled

3.2 Testing of the orthosis

Testing (Figure 4) is carried out in active cooperation between the patient and the technician. The patient is assessed at the frontal and sagittal levels after standing and walking [8]. In this phase the orthosis deficiencies are eliminated, e.g. the degree of dorsal and plantar flexion, the dimensions of the device and the placement of the limb of the orthosis. The test orthosis will be marked with points which are unnecessary in support and may be removed. The openings are important in terms of breathability and overall comfort when wearing the orthosis daily [7].

Figure 4 Testing of the orthosis

3.3 *Production of a definitive orthosis*

The sleeve of the definite knee brace is made to a great extent from composite materials and therefore lamination is used for its production. The auxiliary lines that have been marked on the test sleeves are transferred to the plaster model or, if necessary, made on a positive basis as needed. This is followed by reinforcing the areas that are most stressed with carbon tape (Figure 5). It is mainly the padding of the foot in the plantar part of the heel and the knee in the area of the support areas. Only after checking the position of the splints and reinforcements, does the lamination with laminating resin and hardener continue [7].

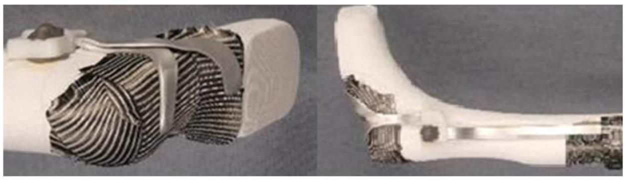

Figure 5 Placing the reinforcing fabric before laminating

The laminating mixture is cured under pressure. After marking the cutting edges, the sleeve is ground and smoothed using a vibrating saw. The laminating tool is removed from the ankle area and replaced with the appropriate ankle insert according to the desired plantar resp. dorsal flexion. The orthosis is completed by fastening through the knee, but also above the ankle, as required (Figure 6) [7].

Figure 6 Definitive knee braces – Subject 1 and subject 2

4 Results of orthotherapy

Prior to the application of the dynamic pre-knee orthosis, a significant valgus of the knees is present in the subject, causing a compensatory position in the ankle joint region. As can be seen, the course of the gravity line in the frontal plane does not correspond to the physiological lines, which is also evident in the symmetrical position of the arms (Figure 7, Figure 8). Prolonged posture with enlarged compensatory lordosis of the lumbar spine and tilt of the pelvis in the PA direction is due to hyperextension of the knee joints and subsequent plantar flexion of the ankles that are observed in the sagittal plane. The gravity line in the sagittal plane in both patients does not run physiologically and affects the maintenance of equilibrium and subsequent stability during standing. This position, however, significantly affects the locomotion pattern of motion and prediction of frequent falls. The following application of dynamic pre-knee orthosis, the following figures clearly show the effect of orthotherapy on body posture, posture stability and hence on locomotion ability. This graphical documentation depicts two polio patients whose medical treatment and rehabilitation have been supplemented by the selection, manufacture and application of a suitable dynamic orthosis. Patients agreed to create photo documentation and its publishing. The pictures on the left show a uniform status of the patient before and after the application of the dynamic orthosis, in the real-life testing process.

Figure 7 Subject 1, anterior, posterior, side view without and with the aid of an applied knee brace.

Figure 8 Subject 2, anterior, posterior, side view without and with the aid of an applied knee brace.

5 Conclusions

The aim of this paper was to describe a particular orthotic solution and optimization of the methodical procedure - design and technological procedure in the application of dynamic knee orthosis for patients after polio. These case studies offer a representative sample of the effect of orthopedic devices. The above-mentioned photo documentation offers an overview and a clear idea of the effect of these orthotic devices. There is an obvious correction of the position of the lower limbs and thus improvement of the overall posture of the individuals. By examining the entire process of designing, developing and applying the orthosis, from the patient's arrival to the prosthetic centre until the definitive orthosis becomes the client's daily aid, one can learn about the results and procedures in orthotic practice.

Acknowledgements
This article was supported by the state grants: VEGA 1/0316/16, KEGA 041TUKE-4/2019 and 023TUKE-4/2020 and APVV-19-0290.

References

[1] MENANT, J., GANDEVIA, S.: *Handbook of Clinical Neurology,* Chapter 21 -Poliomyelitis, Elsevier, Vol. 159, 2018.
[2] ŽIVČÁK, J., et al: *Biomechanika človeka I.,* Human biomechanics I., 1st edition, Prešov, Grafotlač Prešov, 2007. (Original in Slovak)
[3] GENÊT, F., SCHNITZLER, A., MATHIEU, S., AUTRET, K., THÉFENNE, L., DIZIEN, O., MALDJIAN, A.: Orthotic devices and gait in polio patients, *Annals of Physical and Rehabilitation Medicine*, Vol. 53, No. 1, pp. 51-59, 2009. doi:10.1016/j.rehab.2009.11.005
[4] O'CONNOR, J., MCCAUGHAN, D., MCDAID, C., BOOTH, A:, FAYTER, D., RODRIGUEZ-LOPEZ, R., BOWERS, R., DYSON, L., IGLESIAS, C.P., LALOR, S., O'CONNOR, R.J., HILLIPS, M., RAMDHARRY, G.: Orthotic management of instability of the knee related to neuromuscular and central nervous system disorders: Systematic review, qualitative study, survey and costing analysis, *Health technology assessment,* Vol. 20, No. 55, pp. 1-262, 2016. doi:10.3310/hta20550
[5] MORRIS, C., CONDIE, D., (ed): *Recent Developments in Healthcare for Cerebral Palsy, Implications and Opportunities for Orthotics*, Copenhagen, International Society for Prosthetics and Orthotics, 2009.
[6] ARNDT, A., FRÖBERG, Å., MÅRTENSSON, M.: The Effect of Ankle Foot Orthosis' Design and Degree of Dorsiflexion on Achilles Tendon Biomechanics—Tendon Displacement, Lower Leg Muscle Activation, and Plantar Pressure During Walking, *Frontiers in Sports and Active Living*, Switzerland, Frontiers Media SA, Vol. 2, No. March, Article 16, pp. 1-10, 2020. doi:10.3389/fspor.2020.00016
[7] IHNATKO, Ľ.: *Dynamické predkolenné ortézy,* Dynamic below-knee orthesis, Bachelor thesis, Košice, Technical university of Košice, Faculty of mechanical engineering, 2009. (Original in Slovak)
[8] THEODORAKOS, I., RUETERBORIES, J., LUND, M., ANDERSEN, M.S., de ZEE, M., KERSTING, U.G.: Ankle bracing effects on knee and hip mechanics during landing on inclined surfaces, *International Biomechanics*, Vol. 3, No. 1, pp. 22-32, 2016. doi:10.1080/23335432.2015.1132638

Review process
Single-blind peer review process.

doi:10.22306/atec.v6i3.86 Received: 08 June 2020; Revised: 06 Aug. 2020; Accepted: 04 Sep. 2020

INVESTIGATING THE RESTRICTIVE EFFECT OF NEIGHBORING PERFORATION CHANNELS WITH COMPUTATIONAL FLUID DYNAMICS SIMULATION

Ádám V. Pásztor
Petroleum Engineering Department, University of Miskolc, Egyetemváros Miskolc, 3515 Miskolc, Hungary, padamv91@gmail.com (corresponding author)
Zoltán Turzó
Petroleum Engineering Department, University of Miskolc, Egyetemváros Miskolc, 3515 Miskolc, Hungary, turzoz@uni-miskolc.hu

Keywords: CFD simulation, effect of perforation design, flow in porous media, pressure distribution around perforations
Abstract: The inflow performance relationship of a well establishes the link between the applied pressure drawdown and the inflow rate at the bottom of the well. In a cased and perforated well the perforation parameters have a large effect on the inflow performance relationship. When investigating the effect of the different parameters, the most challenging task is to describe the connection between the phase angle of the perforation design and its performance. One of the authors of this paper published a method, which incorporates the perforation channels' restricting effect on the drainage area of each other, which is the function of the phase angle. The aim of this study to validate the restricting effect with the use of computational fluid dynamics (CFD) simulations.

1 Introduction

1.1 Perforation parameters

The perforation channels initiated by a device called perforator gun, which is technically a steel pipe containing many perforator heads filled with some kind of explosive. The perforation process is the conveying of this perforator gun to the desired depth and the firing the explosive (Figure 1).

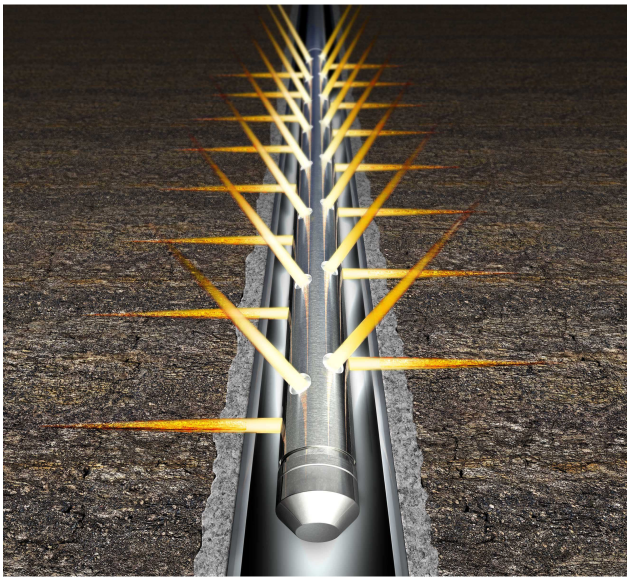

Figure 1 Perforation process
[Source: https://www.halliburton.com/en-US/ps/wireline-perforating/wireline-and-perforating/perforating-services/CHE-System.html, viewed 03 December, 2014]

The perforation design, which is shown on the figure below (Figure 2), is the result of the length of the gun, the type and spatial distribution of the perforator heads and the explosive's type and quantity.

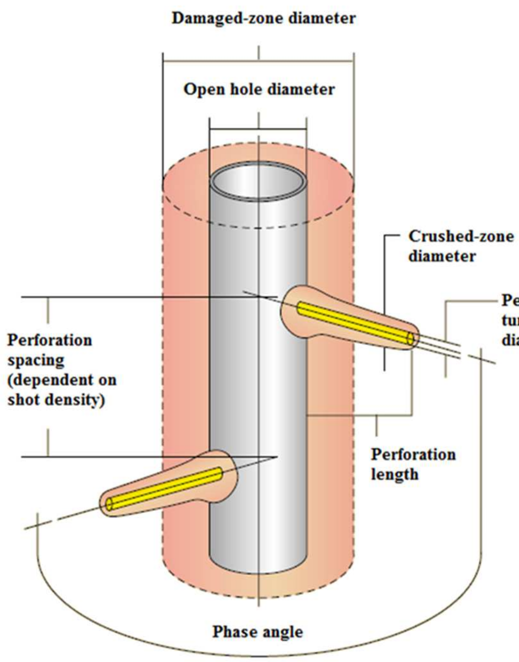

Figure 2 Perforation parameters [1]

The different parameters can be altered by modifying the perforator gun. The commercially available phase angles are presented on the Figure 3.

Acta Tecnología - International Scientific Journal about Technologies
Volume: 6 2020 Issue: 3 Pages: 79-84 ISSN 2453-675X

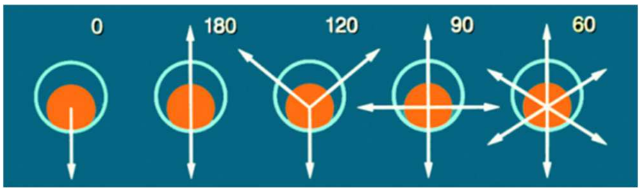

Figure 3 Available phase angles
[Source: https://petrowiki.org/Perforating_design, viewed03 December 2019]

1.2 IPR models for perforated wells

The Inflow Performance Relationship (IPR) of a well describes the change in the inflow in function of the bottom hole pressure, thus it is the perfect mean to investigate the efficiency of a production system.

The relationship between the perforation parameters and the performance of the well is investigated since the 1980s. Yldiz carried out a large-scale investigation on the different available calculation method by checking their accuracy with measured rate independent skin factors [2]. He pointed out, that the two most widely used methods are the method of Karakas and Tariq [3] and the method of McLeod [4].

Karakas and Tariq presented a semi-analytical solution for the skin calculation in perforated completions. They have quantified the wellbore and vertical-flow effects by finite-element simulations. They have showed that the skin effect which is caused by perforations is a combination of four different effects as follows: horizontal skin, vertical skin, wellbore skin, and crushed zone-effects.

McLeod assumed that perforations are small wells in the reservoir and used the Jones [5] method to calculate the pressure drop across them. Unfortunately, this method does not take the effect of phase angle into consideration.

Pásztor and Schultz [1] pointed out in their paper that both of the previously presented methods have some contradictions in their results, thus their application for calculating the IPR of perforated wells is not advised. Based on their further investigation they introduced a new model, which doesn't have the contradictions of its predecessors. Their base concept was to determine the drainage volume around the perforation channels and calculate the productivity of each individual channel accordingly.

2 Restrictive effect of perforation channels

During the filtration from the reservoir to the wellbore there is a well identifiable change in the flow direction from perpendicular to the axis of the well to be perpendicular to the axis of the nearest perforation channel (Figure 4).

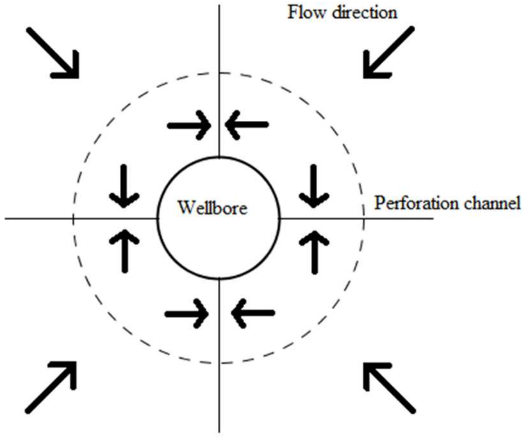

Figure 4 Change in flow direction

The pressure drop during the filtration is proportional to the drainage radius i.e. the furthest point from which fluid flows to the draining point. To the point of direction change this drainage radius is actually the wells drainage radius and the flow to this point is actually a flow to a pseudo well with higher wellbore radius.

After the direction change a flowing particle will flow towards the perforation channel which is the closest to it. The points which are closer to a given perforation than any other, constitutes the drainage volume of the given channel. The closer are the channels to each other the smaller is this volume. This behavior is called the restrictive effect of the perforation channels.

Geometry of the perforations' drainage volume

A perforation channel has six neighboring perforations around it, thus at any given distance from its base there are six points in the perpendicular plane which are equally far from an other perforation. These six points will define an ellipse, which is the boundary of the drainage area at the plane perpendicular to the axis (Figure 5).

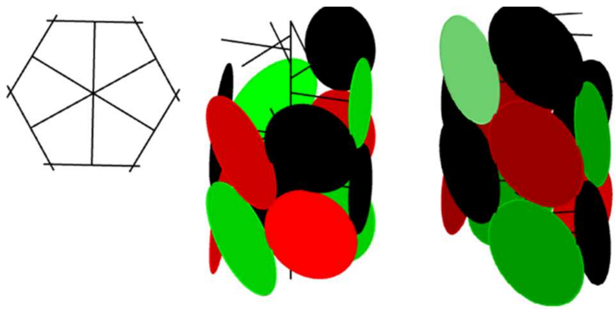

Figure 5 Restrictive effect of perforation channels

The perforation channels are actually evasive straight lines, thus the shape of the drainage space is relatively complex as shown in the figure below (Figure 6).

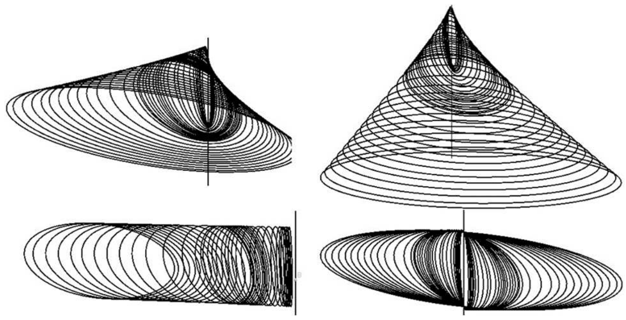

Figure 6 Drainage space of perforation channels

3 CFD model

3.1 Introduction

Computational fluid dynamics techniques provide a way for determining the characteristics of fluid flow around the perforated interwall of a fluid producing well. CFD calculations numerically solve the governing equations for a flowing fluid. To facilitate the simultaneous solution of the governing equations, the procedure involves dividing the flow space into sufficiently small finite volumes or cells [6,7]. The accuracy of flow modeling greatly depends on the proper setup of these cells. This article describes this spatial distribution.

After one properly sets up the cell structure, CFD calculations can determine the pressure distribution, the flow path and flowing velocities etc. in the evaluated domains.

Based on the CFD results, we are validating the assumptions about the change in flow directions and the presence of restrictive effect.

3.2 Basic flow equations

Generally, during CFD simulations, to model the fluid flow the following equations are used.

The Navier-Stokes equation representing Newton's second axiom characterizes flow inside regular fluid domains (flow in . (Equation 1).

$$\frac{\partial \vec{v}}{\partial t} + Div(\vec{v} \circ \vec{v}) = \vec{g} - \frac{1}{\rho} grad p + \vec{v}\Delta\vec{v} + \frac{\mu + \zeta}{\rho} grad\ div\vec{v} \quad (1)$$

where: $\vec{v}$ = velocity vector,
$\vec{g}$ = acceleration gravity vector,
$\boldsymbol{\rho}$ = fluid density,
$\boldsymbol{p}$ = pressure,
$\boldsymbol{\mu}$ = dynamic viscosity,
$\boldsymbol{\zeta}$ = specific viscosity,
$\boldsymbol{t}$ = time.

The continuity equation, Equation 2, describes the conservation of mass, while Equation 3 expresses the conservation of the energy of the flowing fluid.

$$\frac{\partial \rho}{\partial t} + div(\rho\vec{v}) = 0 \quad (2)$$

$$\frac{\partial}{\partial t}\left(\frac{v^2}{2} + h\right)\rho + div\left[\left(\frac{v^2}{2} + h\right)\rho\vec{v} - \lambda\nabla T\right] = \frac{\partial p}{\partial t} \quad (3)$$

where: $\boldsymbol{h}$ = thermodynamic enthalpy,
$\boldsymbol{\lambda}$ = heat conductivity,
$\boldsymbol{T}$ = temperature.

Because these three basic differential equations governing the flow conditions have five unknowns, an unambiguous solution requires two more equations. These are the equation of state for the flowing fluid and the equation describing the change of the enthalpy with the state parameters (Equations 4 and 5).

$$\rho = \rho(T, p) \quad (4)$$
$$h = h(T, p) \quad (5)$$

The five equations constitute a system of equations with five unknowns, making the simultaneous solution of them theoretically possible.

The flow around the well bore is situated in a porous of reservoir rocks (in porous medium) until it reaches the perforations and the well bore. The porous model is the combination of Darcy's law (Equation 6.) commonly used for flows in porous regions and a generalization of the Navier-Stokes equations. This combination can be used to simulate flows if the geometry is too complex to resolve with a grid. The model retains both advection and diffusion terms.

$$\nabla p = -\frac{\mu}{k}\vec{v} \quad (6)$$

where: k = absolute permeability.

During deriving the continuum equations, 'infinitesimal' control volumes and surfaces, large relative to the interstitial spacing of the porous medium, but small relative to the scales wanted to be resolved was assumed. The given control cells and control surfaces are assumed to contain both solid and fluid regions.

3.3 Numerical solution

Because an analytical solution of the basic flow equations (Equations 1-6) is possible only for very simple cases, complex cases usually require numerical solutions, so-called finite element models.

The computational fluid dynamics program package used in this article performs a numerical solution of the governing equations using finite volumes. The program constructs these by dividing the flow space into a finite number of cells with finite volumes connected to each other.

It makes calculations at the geometrical centers of the cells (the node points) and first calculates the fluid and flow parameters. Then it solves the algebraic equations resulting from the integration of the basic differential equations at cell boundaries to obtain the five unknowns at the node points.

3.4 Geometrical flow space model

Results of CFD calculations depend on the proper setup for the geometrical model of the flow space because improper models can cause convergence difficulties and erroneous results. Figure 7a and b. shows the geometrical model of the CFD simulation. In our case, the geometrical model means the representation of reservoir rock around the well and the perforation channels and the well bore. The reservoir rock is a porous domain. The porous domain has cylindrical shape, and in its center the wellbore is located. Both the wellbore and the perforations have cylindrical shapes. The reservoir rock is furtherly divided into two zones. The outer one, the unaltered rock zone. It represents the original reservoir rock. The inner one, the damaged zone, representing the damaged zone due to drilling process. The damaged zone has smaller permeability and porosity than the unaltered zone. There are eight perforations in the model, the phase angel is 90 °. The length of perforations is greater than the damaged zone thickness, it reaches the middle of the unaltered zone, the vertical distance between the perforations at the same angle positions are different for the different angles, to show the effect of it on the inflow behavior. As the figures shows, the whole flow domain is furtherly divided into smaller blocks to help the proper meshing process.

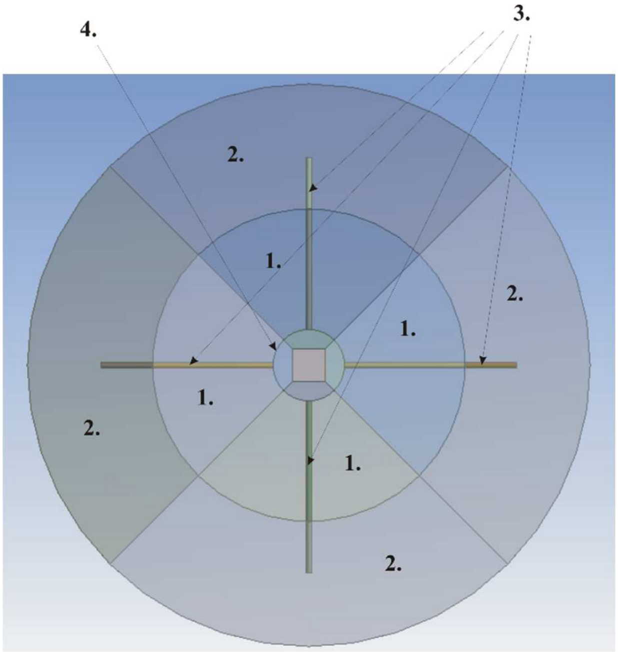

1. Damaged zone; 2. Unaltered zone; 3. Perforations; 4. Wellbore;

Figure 7a Top view of model geometry

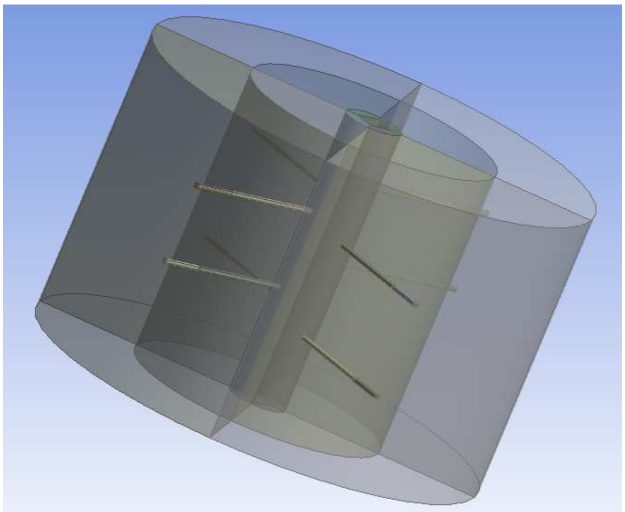

Figure 7b: Isometric view of model geometry

The calculations require the filling of this space with interconnected hexahedrons representing the cells. Ensuring higher accuracies and faster solutions requires selection of the hexahedrons that are nearly cubes.

Figure 8. shows the mesh structure of the fluid domain. One block is hidden on the figure, to show the mesh around perforations, too. The mesh is generated by hex dominant method and includes 491680 elements.

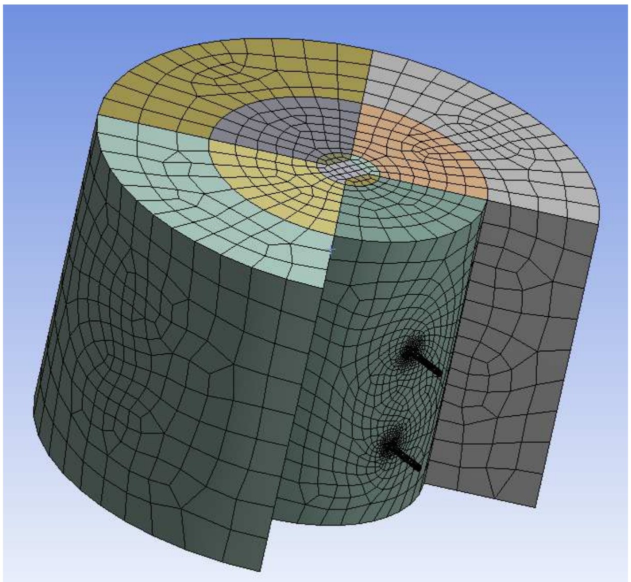

Figure 8 Mesh structure of the model

3.5 Simulation results

The aim of the CFD simulation was to prove the flow direction change near the perforations and to show the restrictive effect of the neighboring perforations. No quantitative analysis made on flow rates.

INVESTIGATING THE RESTRICTIVE EFFECT OF NEIGHBORING PERFORATION CHANNELS WITH COMPUTATIONAL FLUID DYNAMICS SIMULATION
Ádám V. Pásztor; Zoltán Turzó

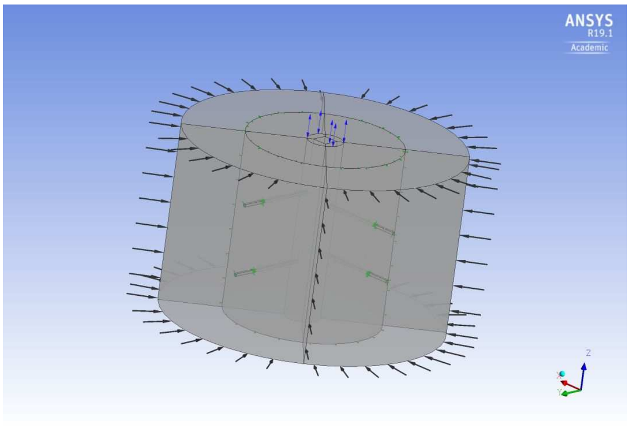

Figure 9 Inlet and outlet ports of the model

Steady state, isotherm flow model with constant pressure boundaries used at inlet and outlet of the flow domain. The Figure 9. shows the inlet and outlet ports of the model. The inlet indicated by black, while outlet by blue arrows. Water flow was modelled while the porous domain 100% saturated by water. Isotropic loss model selected neglecting inertial losses.

The most important results of the simulation for our purpose are the spatial pressure distribution and flowing directions in the model. Figure 10. shows the pressure distribution around perforation channels rendered on some selected planes.

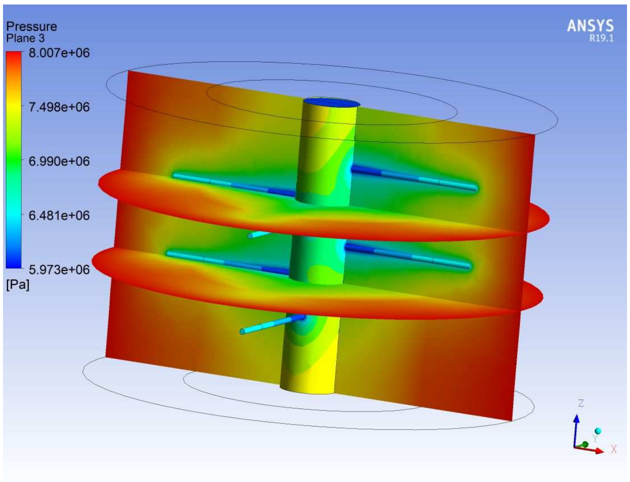

Figure 10 Pressure distribution around perforation channels

Evaluating the results on the figure one can state that the pressure is decreasing towards the perforations. The pressure gradient is higher in the damaged zone than in the unaltered zone. The pressure loss is smaller in the perforations. The pressure profiles around perforations are altered by neighboring perforations. This is the results of restriction effect. The effect is higher for the perforations are closer to each other.

Plotting iso-pressure surfaces around perforations shows the restricting effect much better and illustrates the shape of the flow space around perforations. Figure 11 demonstrate one of the iso-surface of pressure.

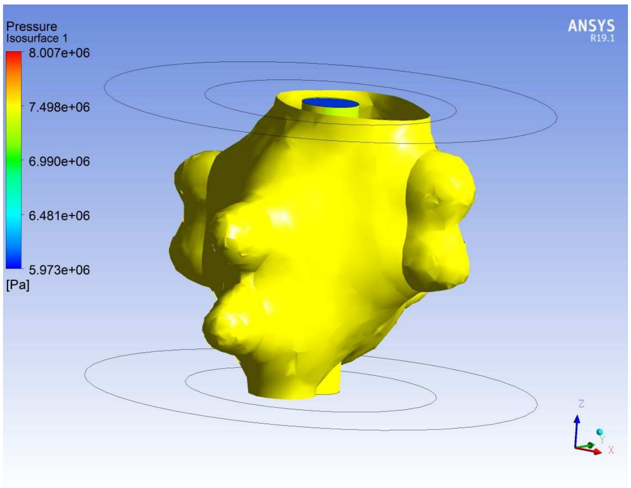

Figure 11 Iso-surface of pressure

Evaluating the shape of the iso-surface, is clear that the restrictive effect is prevail and it is affected by the distance between the perforations. The form of the iso-surface on end of perforations toward the inflow boundary looks like an ellipsoid. It is in sync with our previous statement about elliptical shape of drainage area of perforations.

Another important aspect of the new inflow model for perforated well is the assumption of flow direction change around the perforations. To show the flow directions in the flow space the most convenient way is plotting the streamlines (trajectory) of the flow.

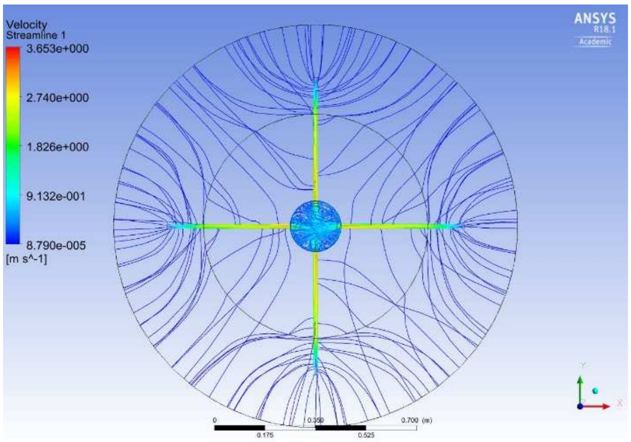

Figure 12 Change in flow direction CFD

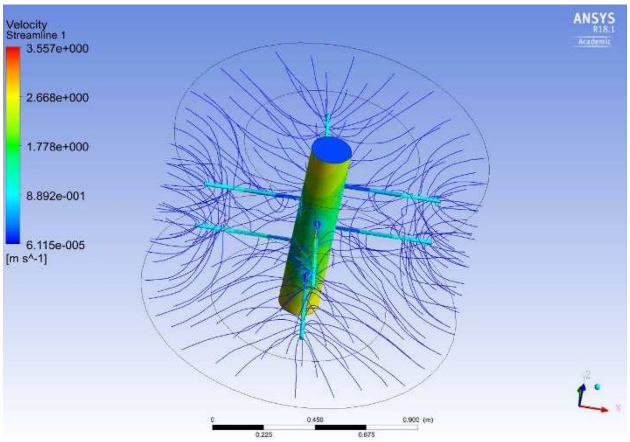

Figure 13 Restrictive effect of perforation channels CFD

Figure 12 and 13. show the propagation of streamlines around the well from two different viewpoints. The streamlines started from the inflow boundary. On the figures, it clearly shown that the flow directions changing around the perforations. The directional change can be identified in both the unaltered and damaged zones. The streamline density is greater in the undamaged zone. It indicates higher flow rates there.

4 Conclusion

The method proposed by Pásztor & Schultz introduced the restrictive effect of neighboring perforation channels as a new concept for calculating the pressure drop of perforates wells. The application of computational fluid dynamics simulation was proven to be the perfect tool to check the validity of the concept.

The results of the CFD simulation provided a series of visual representation of the flow behavior around the perforation channels. The pressure distribution and the pressure iso-surface are good representations of the restrictive effect of adjacent perforation channels. Furthermore, the shape and density of the streamlines and the shape of the pressure iso-surface describe the shape of the drainage area around the perforation channels as well.

- The pressure profiles around perforations are altered by neighboring perforations, which is indicated by the change in the pressure distribution between the perforations.
- The effect is higher for the perforations are closer to each other, which can be seen from the density difference in the streamlines between the vertical and horizontal axis.
- As the flow is perpendicular to the pressure iso-surface, the results are in sync with our previous statement about elliptical shape of drainage area of perforations.

The presented results prove the existence of the restrictive effect and also validates the concept of Pásztor and Schultz about the shape of the drainage areas.

The density of the streamlines is different in the altered and unaltered zones. This behavior indicates that vast portion of the fluid enters the perforation channels in the unaltered zone. This phenomena is crucial regarding the productivity intensification of the wells and its theoretical background was discussed by Pasztor in 2016 [8].

The further investigation of the effect of the altered zone on the flow around the perforated production well with CFD simulations will be the continuation of this research.

References

[1] PASZTOR, A., SCHULTZ, V.: Analytical determination of the perforation design's effect on the productivity, *MOL GROUP Professional Journal,* Vol. 2016, No. 1, pp. 108-117, 2016.
[2] YLDIZ, T.: Assessment of Total Skin Factor in Perforated Wells, *SPE Reservoir Evaluation & Engineering*, Vol. 9, No. 1, pp. 61-76, 2016.
[3] KARAKAS, M., TARIQ, S. M.: Semi-analytical Productivity Models for Perforated Completions, *SPE Production Engineering*, Vol. 6, No. 1, pp. 73-82, 1988.
[4] MCLEOD, O. H. J.: The Effect of Perforating Conditions on Well Performance, *Journal of Petroleum Technology*, Vol. 35, No. 1, pp. 31-39, 1983.
[5] JONES, L. G., BLOUNT, E., GLAZE, O. H.: *Use of Short-Term Multiple-Rate Flow Test to Predict Performance of Wells Having Turbulence*, SPE Annual Technical Conference and Exhibition, New Orleans, 1967.
[6] FERZIGER, J., PERIĆ, M.: *Computational Methods for Fluid Dynamics,* Berlin, Spriger, 2002.
[7] FLETCHER, C.: *Computational Techniques for Fluid Dynamics 1*, Berlin, Springer, 1998.
[8] PÁSZTOR, Á.: *The Invaded Zone's Effect on The Inflow of Perforated Wells*, SPE Hungarian Section, 17. November 2016, [Online] Available: http://hungary.spe.org/viewdocument/spe-hun-conference-2016. [10. Apr. 2020], 2016.

Review process
Single-blind peer review process.

Acta Tecnología - International Scientific Journal about Technologies
Volume: 6 2020 Issue: 3 Pages: 85-88 ISSN 2453-675X

doi:10.22306/atec.v6i3.89 *Received: 18 June 2020; Revised: 21 Aug. 2020; Accepted: 05 Sep. 2020*

THE EFFECT OF MULTI-MATERIAL PRINTING TO FLEXIBILITY

Dominika Belvoncikova
Technical University of Košice, Department of Biomedical Engineering and Measurement, Letna 9, 042 00 Košice, Slovak Republic, EU, dominika.belvoncikova@student.tuke.sk
Lucia Bednarcikova
Technical University of Košice, Department of Biomedical Engineering and Measurement, Letna 9, 042 00 Košice, Slovak Republic, EU, lucia.bednarcikova@tuke.sk
Monika Michalikova
Technical University of Košice, Department of Biomedical Engineering and Measurement, Letna 9, 042 00 Košice, Slovak Republic, EU, monika.michalikova@tuke.sk
Alena Findrik Balogova
Technical University of Košice, Department of Biomedical Engineering and Measurement, Letna 9, 042 00 Košice, Slovak Republic, EU, alena.balogova@tuke.sk
Eduard Jakubkovic
Technical University of Košice, Department of Biomedical Engineering and Measurement, Letna 9, 042 00 Košice, Slovak Republic, EU, eduard.jakubkovic@tuke.sk
Marianna Trebunova
Technical University of Košice, Department of Biomedical Engineering and Measurement, Letna 9, 042 00 Košice, Slovak Republic, EU, marianna.trebunova@tuke.sk (corresponding author)

Keywords: flexibility; materials; bending; 3D printing
Abstract: Currently, 3D printing is one of the popular technological production methods, mainly because it offers various options that affect the resulting properties of prints. The aim of the presented work is to manufacture a prosthetic finger with a PIP and DIP joint using multi-material 3D printing, which will allow to mimic the flexion of a physiological finger. The subject of this research and testing is the design of a combination of solid and flexible material for a monolithic finger model, which will allow the required bending in selected areas of the print.

1 Introduction

Additive manufacturing (AM), which is based on layer-by-layer material addition, provides an opportunity for producing multi-material components with customized geometry tailored material properties at different locations and tailored functionality. Current developments in Multiple Material Additive Manufacturing (MMAM) focus mainly on producing components with similar material properties [1,2], such as those consisting of polymer-polymer [3-5]; polymer composite with nano-and micro-particle filler [6,7]; metal-metal [8,9]. In the field of prosthetics and orthotics in the design of prostheses, orthoses and other aids, it is very important to choose a suitable material, resp. combinations of materials. This choice of different materials makes it possible to influence the resulting properties of the product, e.g. flexibility. The presented study deals with the selection of a suitable combination of materials for the production of a prosthetic finger model, which will allow the most realistic flexion of its individual links in the area of joints. Combination of suitably selected materials results in better properties and lower maintenance requirements for the prosthesis. The aim was to ensure sufficient flexibility of the printout, which was to be achieved by using a flexible material, with sustainability of the printout shape and ensuring bending in the desired direction, which ensured the choice of rigid material.

2 Material and methods

The design of a functional monolithic prosthetic finger consists of 3 segments, which are connected to each other by a PIP and a DIP joint. This model is designed as one piece, where different combinations of materials are in the areas of joints in order to achieve the most natural flexion. Two types of 3D printers were used for the additive manufacturing, which enable multi-material printing, namely the TEVO Tarantula - Prusa i3 printer and the Bioplotter Manufacturer. Hobby printer TEVO Tarantula is an FDM type that prints the filament supplied in the spool layer by layer by building on a bitmap according to a CAD model [10]. The second type is the Bioplotter Manufacturer dual printer with the possibility of printing low-temperature and high-temperature material. PLA (polylactic acid), TPE-E (thermoplastic elastomer) and LSR (silicone) were chosen as printing materials due to their suitable properties (Table 1) [11].

Table 1 Properties of selected material filaments

	TPE	PLA	LSR
Tensile strength	26-43 MPa	65 MPa	7 MPa
Brittleness	1/10	7,5/10	>1/10
Thermal expansion coefficient	157µm/m-°C	68µm/m-°C	250 µm/m-°C
Density	1,19-1,23 g/cm³	1,24 g/cm³	1,10-1,50 g/cm³
Printability	6/10	9/10	5/10
Flexibility	high	low	high
Elasticity	high	low	extremely high
Impact resistance	high	low	medium
Fatigue resistance	high	very low	very high
Thermal resistance	low	low	low
Shrinkage	low	low	low
Recyclability	Y	Y	N
Bioabsorption	Y	Y	N
Biocompatibility	Y	Y	Y
Chemical resistance	Y	N	Y

3 Experiment

The experimental part deals with the combination of 3D printing of solid and flexible materials and their influence on bending. A key feature for achieving prosthetic finger flexion is the elasticity of the material. Elasticity in structural mechanics means that the material responds elastically to an applied load and when the load is removed it returns to its original shape. Flexibility is less well defined but means that the material will respond to loading by deforming without fracture but does not necessarily fully return to its original shape. The Young's modulus parameter, which is based on Hooke's law, was used to analyse the property. It describes the relationship between the deformation of a solid body caused by the action of stress and its magnitude.

Table 2 The degree of elasticity of materials according to Young's modulus

Material	Young's module	Flexibility
PLA	3 500 MPa	Low flexibility
TPE - FilaFlex	95 MPa	High flexibility
TPE - Arnitel	250 MPa	Semi-flexibility
Silicone	3,3 MPa	High flexibility

In the first part of the experiment the combination of printing of low-temperature and high-temperature materials were verified. It was used a multi-cartridge printer Bioplotter Manufacturer. As a less flexible material with a high melting point, was chosen a mixture of PLA and PHB, which has the desired properties. The highly flexible low melting point material was Mapei's LSR silicone from Mapesil.

Table 3 The degree of elasticity of materials according to Young's modulus

	Layer number	Layer order	Material	Dimension	Position
A	3	1. 3. 5.	PLA	10x60 mm	Whole model
B	2	3. 4.	PLA	10x25 mm	Proximal part of specimen
C	2	3. 4.	LSR	10x10 mm	Joint part of model
D	1	2. 4.	PLA	10x25 mm	Distal part of specimen

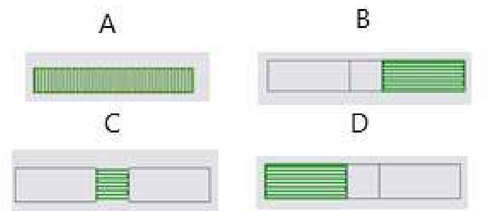

For the purpose of our research work were made three specimens, which were modelled in Autodesk Meshmixer program. The first sample is in the shape of a square with dimensions of 20x20*mm*. It is a four-layer model, where the layers alternate in the order PLA, LSR, PLA, LSR. Sample No. 2 was designed to resemble the actual flexion of the finger, so the rigid parts are connected to each other via flexible joint parts. The combination of materials was only in the articulated part, where PLA alternates with LSR with the intention to increase the flexibility of the transition. Our designed model consisted of layering prisms PLA (low flexibility) and LSR (high flexibility), where the first, third, fifth layer is formed by PLA prism with dimensions 20x60*mm* and a second and fourth layer of LSR prisms with dimensions of 20x20*mm*. The square in the middle represents the joint, so it should provide the greatest flexibility during the bending. The ribbing of the lamellae during the alternation of the individual layers over the entire surface of the print is formed by the structure of the grid. The third sample was created by dimensional modification of sample no. 2. The design was based on the assumption that the narrowing of the layers will ensure better adhesion between the layers [12,13]. Dimensions of sample no. 3 are listed in Table 3.

4 Results

During the experiment, the adhesion between their individual layers is the biggest problem with the prints made of several materials. Silicone only binds to another silicone or LSR. Another problem is that the Bioplotter can print multiple material filaments at the same time, but the materials must belong to different groups in terms of their printing temperature. For these reasons, the type of LSR and PLA or other high-temperature material used was evaluated as unsuitable bonding materials. The experiment further showed that the reason for the lack of adhesion between the silicone and the PLA mixture is the presence of hydrogen bonds in the chemical structure of the silicone, which weaken the ionic and covalent bonds necessary for the cohesion of the layers.

Specimen no. 1 was necessary to print with a contour, because of an unsuitable bend occurs around the z-axis. The flexibility of this sample is sufficient for the needs of the experiment, but the persistent problem of layer adhesion precludes its use.

In the second specimen, it can be seen that the linear lines of the structure overlap and a grid is formed. This and conjunction with the alternation of the filament materials, provides the desired bend in the joint area and not outside it. However, the most serious drawback is the adhesion of the layers of different materials, and there was also the breakage of the lamellae at the bending point.

The design of specimen no. 3 was approached in order to eliminate the lack of adhesion between the layers. The dimensions were modified and the last LSR layer was covered with a PLA layer (Figure 1). Although greater cohesiveness between the layers was visible in the bending test, it was found that the problem of adhesion was not eliminated. In this sample, an increased brittleness of the material is observed compared to the previous one. The lamellae break not only at the junction of the contour and the ribbing, but also in the area of the ribbing itself and, to the greatest extent, on the side which was printed out first.

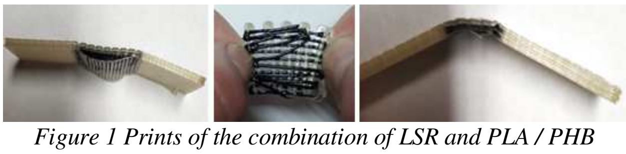

Figure 1 Prints of the combination of LSR and PLA / PHB mixture, Left - first specimen, second specimen, third specimen

5 Discussion

Flexibility as a property describes the relationship between the deformation of a solid body caused by stress and its magnitude. The higher the Young's modulus, the greater the stress required to achieve the same deformation [14].

In the process of combining materials, the addition of PHB to the PLA mixture ensures an improvement in post-process stability by 20% compared to pure PLA [15]. This mixture also shows better properties in terms of material flexibility. In the combination of LSR and PLA / PHB, the biggest problem was the lack of adhesion between the layers. This is because of the intermolecular adhesive forces of silicone are weak. Although the angle between the PLA and the silicone was in the range of 0 °-45 °, the layers held together only by solidification and mutual pressure. It should be noted that this material does not adhere to other materials due to its chemical structure. Ionic and covalent forces are important for adhesion. Due to the hydrogen bond present in the silicone molecule, these bonds are weakened. Thus, the ionic and covalent bonds between the silicone molecules and the PLA + PHB mixture are not strong enough to provide the desired interlayer adhesion [10]. This insufficiently strong bond thus results in poor cohesion of the silicone and PLA mixture layers used in the experiment. To improve this problem, it is recommended to use a combination of silicone with silicone or a PLA mixture with materials that bond well with it or another printing method.

The biggest problem was the jamming of the filament in the extruder, which resulted in its unusability in printing, when testing the TPE-U Filaflex and when testing the flexibility of the printout. This was caused by the flexibility of the coil. The utilisation this material or any other material with a comparable modulus of elasticity for manufacturing, it is necessary to specifically adjust the print settings for a particular printer. Printing with TPE Arnitel proved to be suitable. The reason for the better printing process than the TPE-U variant was the higher value of the Young's modulus. The higher the Young's modulus of the material, the greater the stress required to achieve the same deformation [14].

The next possible solution could be to replace the LSR material (the group of acetic silicones), with a hybrid (acetic-neutral cured) silicone, which provides better adhesive properties. Such a material could be a polyether adhesive - ChemSet MS - 10. This material is used as a substitute for acetic silicone where a stronger binder is needed for industrial applications while maintaining the flexible properties offered by the LSR material group.

Another solution would be to replace both materials. It can be used a high-temperature material for the Bioplotter, for example ABS, which bonds well with the TPE material. An example of a suitable elastomer would be Polabond series 6401-6402, which would be exchanged for the LSR used [16].

6 Conclusion

The aim of the presented work was to imitate the flexion of the finger. It was based on the null hypothesis that the combination of solid and flexible material could result in flexion of the finger prosthesis. For this purpose, the Bioplotter multi-material printer was chosen as one of the manufacturing options. The selected materials were a mixture of PLA and PHB and LSR of the sanitary silicone type. The hypothesis was not confirmed due to the fact that the adhesion between the layers of materials with a different chemical structure was not sufficient.

FDM printing of the materials described above has proven successful. TEVO Tarantula - Prusa i3 printer was used to print specimens from Arnitel and Filaflex. This variant is very suitable for printing simple and small designs, as it has a printing bed with dimensions of 200mm x 200mm x 200mm. This platform is even heating and can be set from 60 to 120 °C. It can print models from materials such as PLA, ABS, PTEG, wood filament, TPE, PVE. The smallest possible layer thickness is 50 microns with a nozzle diameter of 1.75 mm and a print speed of 150 *mm/s* [10].

Acknowledgement

The manuscript has been supported by research grants: Stimulus for Research and Development of Ministry of Education No. 1233/2018, Cultural and educational grant agency of the Ministry of Education, Science, Research and Sports of the Slovak Republic: KEGA 041TUKE-4/2019, KEGA 023TUKE-4/2020, KEGA 006STU-4/2018, Agency of the Ministry of Education, Science, Research and Sport of the Slovak Republic and the Slovak Academy of Sciences:VEGA 1/0316/18, VEGA 1/0179/19 and Research and Development Support Agency APVV-19-0290, APVV-17-0278.

References

[1] VAEZI, M., CHIANRABUTRA, S., MELLOR, B., YANG, D.S.: Multiple material additive manufacturing – Part 1: a review, *Virtual and Physical Prototyping,* Vol. 8, No. 1, pp. 19-50, 2013.

[2] BANDYOPADHYAY, A., HEER, B.: Additive manufacturing of multi-material structures, *Materials Science and Engineering: R: Reports*, Vol. 129, No. July, pp. 1-16, 2018.

[3] CHOI, J.W., KIM, H.C., WICKER, R.: Multi-material stereolithography, *Journal of Materials Processing Technology,* Vol. 211, No. 3, pp. 318-328, 2011.

[4] ZHOU, C.Y., EPSTEIN, B.K.: *Development of a multi-materialmask-image-projection-based stereolithography for the fabrication of digital materials,* 22nd Annual International Solid Freeform Fabrication Symposium - An Additive Manufacturing Conference, SFF 2011, pp. 65-80, 2011.

[5] GRÄFE, D.A., WICKBERG, A., ZIEGER, M.M., WEGENER, M., BLASCO, E., BARNER-KOWOLLIK, CH.: Adding chemically selective subtraction to multi-material 3D additive manufacturing, *Nature Communications,* Vol. 9, No. 1, pp. 1-6, 2018. doi:10.1038/s41467-018-05234-0

[6] CHUNG, H., DAS, S.: Functionally graded Nylon-11/silica nanocomposites produced by selective laser sintering, *Materials Science and Engineering: A*, Vol. 487, No. 1, pp. 251-257, 2008.

[7] SINGH, R. N., AMENDOLA, A., FRATERNALI F.: On the wear properties of Nylon6-SiC-Al2O3 based fused deposition modelling feed stock filament, *Composites Part B: Engineering*, Vol. 119, p. 125-131, 2017.

[8] WEI, C., L. Li, ZHANG, X., CHUEH, Y.-H.: 3D printing of multiple metallic materials via modified selective laser melting, *CIRP Annals*, Vol. 67, No. 1, pp. 245-248, 2018.

[9] KOOPMANN, J., VOIGT, J., NIENDORF, T.: Additive Manufacturing of a Steel–Ceramic Multi-Material by Selective Laser Melting, *Metallurgical and Materials Transactions B,* Vol. 50, pp. 1042-1051, 2019.

[10] TEVO, *TEVO TEVO Tarantula I3*, [Online], Available: https://www.treatstock.com/machines/item/297-tevo-tarantula-i3 [2020-05-05] 2020.

[11] EnvisionTEC 3D-Bioplotter Manufacturer Series. Nano-Engineering Research Core Facility (NERCF), [Online], Avaliable: https://engineering.unl.edu/nercf/envisiontec-3d-bioplotter-manufacturer-seriesz [2019-04-09].

[12] VON FRAUNHOFER, J.A.: Adhesion and Cohesion, *International Journal of Dentistry*, Vol. 2012, pp. 1-8, 2012. doi:10.1155/2012/951324.

[13] HARRIS, C.G., JURSIK, N.J.S., ROCHEFORT, W.E., WALKER, T.W: Additive Manufacturing with Soft TPU – Adhesion Strength in Multimaterial Flexible Joints, *Frontiers in Mechanical Engineering,* Vol. 5, No. 7, pp. 1-6, 2019.

[14] TREBUŇA, F., ŠIMČÁK, F.: *Pružnosť, pevnosť a plastickosť v strojárstve,* Košice, Emilena, 2005. (Original in Slovak)

[15] ALEXY, P., CHODAK, I.: *Biodegradable materials based on PLA, PHB and their blends,* Trends in Bioplastics, Ljubljana (Slovinsko), 2014, [Online]. Available: http://www.plastice.org/home/ [2019-04-01], 2014.

[16] RTP Co., *TPE Overmolding, Bonding and Substrate Considerations*, [Online], Available: https://www.rtpcompany.com/products/elastomer/tpe-overmolding-bonding-and-substrate-considerations [2020-05-05] 2020.

Review process

Single-blind peer review process.

JOURNAL STATEMENT

Journal name:	**Acta Tecnología**
Abbreviated key title:	Acta Tecnol
Journal title initials:	AT
Journal doi:	10.22306/atec
ISSN:	2453-675X
Start year:	2015
The first publishing:	October 2015
Issue publishing:	Quarterly
Publishing form:	On-line electronic publishing
Availability of articles:	Open Access Journal
Journal license:	CC BY-NC
Publication ethics:	COPE, ELSEVIER Publishing Ethics
Plagiarism check:	Worldwide originality control system
Peer review process:	Single-blind review at least two reviewers
Language:	English
Journal e-mail:	**info@actatecnologia.eu**

The journal focuses mainly for the original and new, interesting, high-quality, theoretical, practical and application-oriented contributions to the field of science and research as well as to pedagogy and education in the field of technologies.

Publisher:	**4S go, s.r.o.**
Address:	Semsa 24, 044 21 Semsa, Slovak Republic, EU
Phone:	+421 948 366 110
Publisher e-mail:	**info@4sgo.eu**

Responsibility for the content of a manuscript rests upon the authors and not upon the editors or the publisher.